0 0 0 0 4 2 0 4 1 7 2

LBL-3350

c.1

HIGHER ORDER VACUUM POLARIZATION FOR FINITE RADIUS NUCLEI: APPLICATION TO MUONIC Pb AND HEAVY ION COLLISIONS

Miklos Gyulassy
(Ph. D. thesis)

September 25, 1974

Prepared for the U. S. Atomic Energy Commission
under Contract W-7405-ENG-48

For Reference

Not to be taken from this room

LAWRENCE BERKELEY LABORATORY
UNIVERSITY OF CALIFORNIA
BERKELEY

LBL-3350
c.1

DISCLAIMER

This document was prepared as an account of work sponsored by the United States Government. While this document is believed to contain correct information, neither the United States Government nor any agency thereof, nor the Regents of the University of California, nor any of their employees, makes any warranty, express or implied, or assumes any legal responsibility for the accuracy, completeness, or usefulness of any information, apparatus, product, or process disclosed, or represents that its use would not infringe privately owned rights. Reference herein to any specific commercial product, process, or service by its trade name, trademark, manufacturer, or otherwise, does not necessarily constitute or imply its endorsement, recommendation, or favoring by the United States Government or any agency thereof, or the Regents of the University of California. The views and opinions of authors expressed herein do not necessarily state or reflect those of the United States Government or any agency thereof or the Regents of the University of California.

0 0 0 0 4 2 0 4 1 7 3

HIGHER ORDER VACUUM POLARIZATION FOR FINITE RADIUS NUCLEI: APPLICATION TO MUONIC Pb AND HEAVY ION COLLISIONS

Miklos Gyulassy

CONTENTS

PAGE

Abstract iii

Introduction v

Chapter I: Nuclear Size Effects on Vacuum Polarization in Muonic Pb 1

Chapter II: Vacuum Polarization in Heavy Ion Collisions 14

Chapter III: Higher Order Vacuum Polarization for Finite Radius Nuclei 27

Acknowledgments 89

HIGHER ORDER VACUUM POLARIZATION FOR FINITE RADIUS NUCLEI: APPLICATION TO MUONIC Pb AND HEAVY ION COLLISIONS

Miklos Gyulassy

Lawrence Berkeley Laboratory
University of California
Berkeley, California 94720

September 25, 1974

ABSTRACT

This dissertation is concerned with vacuum polarization in the field of finite radius nuclei. In particular, the higher order, $\alpha(Z\alpha)^n$, $n \geq 3$, vacuum polarization charge density is studied. The Wichmann-Kroll formalism relating the vacuum polarization charge density to the Green's function of the Dirac equation is reviewed, and the modifications necessary for very large Z systems with $Z > 137$ are discussed. The radial Green's functions for the Dirac equation in the field of finite radius nuclei are constructed and the higher order vacuum polarization charge density, ρ^{3+}, is calculated numerically from those Green's functions. The third order vacuum polarization charge density, ρ^3, is calculated separately using the third order radial Green's function in order to provide a check on the calculation of ρ^{3+} and to estimate the dependence ρ^{3+} on different models for the nuclear charge density. The nuclear size effect is calculated explicitly for only the lowest angular momentum $(j = \frac{1}{2})$ contribution to the vacuum polarization density. The effect on the contribution from higher angular momentum $(j \geq \frac{3}{2})$ is estimated from the known results for point nuclei. Specific calculations are made for muonic Pb and for superheavy electronic atoms. For muonic Pb the energy level

shifts due to ρ^{3+} and ρ^{3} on high angular momentum states ($5g_{9/2}$, $4f_{7/2}$, $3d_{5/2}$) are calculated in view of reported discrepancies between theory and experiment. The point nucleus limit is checked against known results, and the finite size effects are compared with other calculations. Also, the accuracy of previous approximate calculations based on the smallness of the electron mass and of the nuclear radius are investigated numerically. For superheavy electronic atoms, the problem of whether the higher order vacuum polarization can prevent the $1S_{1/2}$ state from reaching the lower continuum, $E = -m_e c^2$, for some critical charge $Z_{cr} > 137$ is investigated. The charge density of the overcritical vacuum is then calculated and the stability and localization of a helium-like system for Z in the neighborhood of Z_{cr} is studied.

0 0 0 0 4 2 0 4 1 7 4

INTRODUCTION

The three papers that comprise this dissertation present the results of a study of the nuclear size effects on higher order vacuum polarization. The first two papers, Chapters I and II, present specific results for muonic Pb and superheavy electronic atoms. The last paper, Chapter III, presents the general discussion of the calculation of the higher order vacuum polarization density, ρ^{3+}, and the specific details and methods used in arriving at the conclusions reported in the first two papers.

Chapter I is organized as follows: Reasons are given why the calculation of ρ^{3+} for finite radius nuclei is of interest in connection with muonic Pb. Then the approximation obtained by calculating the nuclear size effect for only the lowest angular momentum ($j = \frac{1}{2}$) contribution to ρ^{3+} is made, and the size of the contribution from $j \geq \frac{3}{2}$ is estimated from the results of Wichmann and Kroll. For this estimate, the vacuum polarization charge accumulated at the origin for the case of point nuclei is calculated for the $j = \frac{1}{2}$ contribution to the third order density ρ^3. Then, the results of the energy level shifts due to ρ^3 and ρ^{3+} in the limit of a point nucleus are compared to known results for the $5g_{9/2}$ and $4f_{7/2}$ muonic levels. The finite size effects are investigated first for the third order density ρ^3, and the dependence of these effects on the nuclear charge density, ρ_{Nuc}, is studied by calculating ρ^3 with two different models of ρ_{Nuc}. The higher order density ρ^{3+} is then calculated with the simplest model, $\rho_{Nuc} = \delta(r - R)/4\pi R^2$, where R is chosen to equal the root mean square radius of Pb as determined

experimentally. Finally, the accuracy of the approximation used by other workers in analytic calculations of the finite size effect on ρ^{3+} is studied.

In Chapter II, the results for very large Z systems encountered in heavy ion collisions are discussed. First, the reasons why we may expect a rapid increase in the effect of higher order vacuum polarization for $Z > 137$ are given. Then the approximation obtained by neglecting the $|k| \geq 2$ contribution to ρ^{3+} is justified. Specific calculations of ρ^{3+} and ρ^{3} for $Z \to Z_{cr} \sim 170$ are made in order to see if (higher order) vacuum polarization can prevent the $1S_{1/2}$ electronic state from reaching the lower continuum, $E = -m_e c^2$, for $Z = Z_{cr}$. The tests made to determine the accuracy of the computed bound state wavefunctions and ρ^{3+} are then described. The dependence of the $1S_{1/2}$ energy shift on the different models of ρ_{Nuc} is then estimated as in Chapter I by calculating ρ^{3} with two different models of ρ_{Nuc}. For $Z > Z_{cr}$, the relation of ρ^{3+} to the helium-like density ρ_{He} is discussed. The helium-like density is then calculated for $Z < Z_{cr}$ and $Z > Z_{cr}$, and the continuity and localization of ρ_{He} are examined in detail for Z in the neighborhood of Z_{cr}.

In Chapter III, the formal relations between the Green's function for the Dirac equation and the vacuum polarization density are reviewed, and the regularization of those relations is discussed. The radial Green's functions are constructed for finite radius nuclei. Expressions valid to all orders in $Z\alpha$ as well as for terms of first and third orders are given. Then, the results for muonic Pb and superheavy electronic atoms are further elaborated upon. In particular, the effect of finite nuclear size on the vacuum polarization density

0 0 0 0 4 2 0 4 1 7 5

itself is discussed in order to supplement the discussion of the first two chapters, where the emphasis was on the resulting energy shifts. Finally, the numerical techniques employed in the calculation of the radial Green's functions and of the vacuum polarization charge densities are discussed.

0 0 0 0 4 2 0 4 1 7 6

CHAPTER I

NUCLEAR SIZE EFFECTS ON VACUUM POLARIZATION IN MUONIC Pb

Phys. Rev. Letters 32, 1393 (1974)

NUCLEAR SIZE EFFECTS ON VACUUM POLARIZATION IN MUONIC Pb *

M. Gyulassy

Lawrence Berkeley Laboratory
University of California
Berkeley, California 94720

April 22, 1974

ABSTRACT

The effect of finite nuclear size on the vacuum polarization charge density is studied. The results to third order, $\alpha(Z\alpha)^3$, and to all orders, $\alpha(Z\alpha)^{n\geq 3}$, are presented with special attention focused on the $5g_{9/2} - 4f_{7/2}$ transition in muonic Pb. In addition, the accuracy of analytic calculations exploiting the smallness of the electron mass and of the nuclear radius is discussed.

One of the major tests of quantum electrodynamics lies in the calculation of transition energies in high-Z muonic atoms. The most important radiative corrections to these transition energies come from vacuum polarization (VP). Even the higher-order, $\alpha(Z\alpha)^{n\geq 3}$, VP is important due to the high resolution of recent experiments. Since discrepancies between theory and experiment have been observed,[1] most notably in Ba_{56} and Pb_{82}, several workers[2,3,4] have looked at the higher-order VP in more detail. In particular, the effect of finite

nuclear size on the VP charge density has been studied. However, complete agreement on the size of this effect has not yet been reached. In the hope of eliminating this uncertainty, this letter presents the results of an independent numerical study of the problem.

In muonic Pb, a 42 ± 20 eV discrepancy[3] exists between theory and experiment for the $5g_{9/2} - 4f_{7/2}$ transition when the theoretical contribution to the transition energy due to higher-order VP is calculated for a point nucleus. For a finite size nucleus, characterized by a radius R, the VP charge density, $\rho(R,r)$, differs from its point nucleus form in such a way as to increase the transition energy. This has the effect of increasing the discrepancy between theory and experiment. For the $5g - 4f$ transition this increase was calculated numerically by Rinker and Wilets[2] to be 16 eV. On the other hand, the analytic calculations of Arafune[3] and Brown, et al.[4], using the approximations based on the smallness of m_e and the ratio of the nuclear radius to the muonic orbit, R/a_0, gave 5 eV.

The calculation reported in this letter gives 6 eV for the energy shift of the $5g - 4f$ transition. The central assumption in this calculation is that the finite nuclear size is felt only by the $j = \frac{1}{2}$ electrons in the VP density. It is shown that this assumption leads to an error of less than 0.5 eV for the 6 eV calculated. The third order, $\alpha(Z\alpha)^3$, contribution and the contribution to all orders, $\alpha(Z\alpha)^{n \geq 3}$, are studied separately. This provides a check on the internal consistency of the final results since the numerical techniques required to calculate each are quite distinct. As a further check, the

point nucleus limit, $R \to 0$, is examined and compared to the results of Wichmann and Kroll[5] and of Blomqvist[6]. Finally, setting $m_e = 0$ and expanding to lowest order in R/a_0 in our calculation, we recover the 5 eV result of Refs. 3 and 4.

Wichmann and Kroll[5] showed that $\rho(R,r)$ is proportional to a contour integral along the imaginary energy axis of the trace of the Green's function, $\mathrm{Tr}G(\tilde{r},\tilde{r};z)$, for the Dirac equation. Expanding G in terms of the radial Green's functions, G_k, for "angular momentum," $k = \pm(j + \frac{1}{2})$, we define the VP density, ρ_k, for a given k, through the contour integral of $\mathrm{Tr}G_k$. The radial Dirac equation for G_k may be converted to an integral equation from which a power series expansion of G_k in powers of $Z\alpha$ is obtained. In this way the Uehling term, ρ^1_k, and the third order density, ρ^3_k, may be isolated. Since the $k = \pm 1(S_{1/2}, P_{1/2})$ states are most sensitive to nuclear size, a natural approximation for $\rho(R,r)$ is

$$\rho(R,r) \cong \rho_{|k|=1}(R,r) + \sum_{|k|\geq 2} \rho_{|k|}(0,r) \; ; \qquad (1)$$

i.e., the energy shift due to finite size effects on VP is assumed to come mainly from the $|k| = 1$ density. The accuracy of this approximation depends on how large the contribution from the $|k| \geq 2$ density is. The size of the $|k| \geq 2$ contribution to the total density can be estimated using the results of Ref. 5 for a point nucleus. The ratio, $Q_{k\geq 2}/Q_{k=1}$, of the VP charge accumulated at the origin for $|k| \geq 2$ and for $|k| = 1$ gives a measure of the relative size of $\rho_{k\geq 2}$ to

to $\rho_{k=1}$. For order $(Z\alpha)^{n\geq 5}$, in Pb, Ref. 5 gives $Q^{5+}_{k\geq 2}/Q^{5+}_{k=1} \sim 0.008$ with $Q^{5+}_{k=1} = -6.83 \times 10^{-4}|e|$. From this we conclude that the $|k| \geq 2$ contribution to the density is less than 1% for these orders. For third order, Ref. 5 gives the charge summed over k: $Q^3_{WK} = -4.487 \times 10^{-3}|e|$. To calculate what fraction of Q^3_{WK} comes from $|k| = 1$, we calculated $\rho^3_{k=1}$ numerically using the integral equation for $G^3_{k=1}$ in which we set $m_e = 0$. The nuclear charge distribution used in the calculation was a shell of radius R. The $m_e = 0$ limit isolates the piece of ρ^3_1 which is only a function of r/R. It is precisely this piece that reduces to a delta function as $R \to 0$. (This assumes that the integral of ρ^3_1 over all space exists, which is the case here.) The third order charge due to $|k| = 1$ is then

$$Q^3_1 = \int_0^\infty dr\, 4\pi r^2\, \rho^3_1(R,r,m_e=0) \,. \tag{2}$$

Note that Q^3_1 is in fact independent of R. This was checked numerically by calculating Q^3_1 for R = 6., 0.6, 0.06 F with the result in each case being $Q^3_1 = -4.177 \times 10^{-3}|e|$. Thus $Q^3_1/Q^3_{WK} = 0.93$; i.e., 7% of the third order density comes from $|k| \geq 2$. Summarizing these relations,

$$Q^3_{k=1} \cong 13.5\, Q^3_{k\geq 2} \cong 6.12\, Q^{5+}_{k=1} \cong 770\, Q^{5+}_{k\geq 2} \,. \tag{3}$$

For the case of a point nucleus Blomqvist[6] has calculated the 5g - 4f energy shift in Pb due to third order VP to be $\Delta E^3(R=0) = -43$ eV. For a finite size nucleus we calculated $\rho^3_1(R,r)$ numerically with $m_e \neq 0$ using two different models of the nuclear

charge density: (I) a shell density, $\rho_{nuc} = \delta(r - R)/(4\pi R^2)$ and (II) a uniform density, $\rho_{nuc} = \theta(R - r)/(4\pi R^3/3)$. Tables I and II contain the results. The $R \to 0$ limit was examined by calculating the energy shifts for $R = 0.6$ and 0.06 F. Extrapolating to $R = 0$, we get $\Delta E^3_{k=1} = -40$ eV for the 5g - 4f transition. From Eq. (3) we estimate the $|k| \geqslant 2$ contribution to be $\Delta E^3_{k\geqslant 2} = -3$ eV. Thus, $\Delta E^3_{k\geqslant 1} = -43$ eV, in agreement with Ref. 6. For the calculation of the finite size effect, R was chosen in each model so that $\left[\langle r^2\rangle_{nuc}\right]^{\frac{1}{2}} = 5.5$ F.[7] Dirac wave functions were used in the expectation values, although Schrodinger wave functions gave the same results to within 1 - 2%. (It should be noted that the uncertainty in the muon mass, $\pm$ 400 eV, alone generates a $\pm$ 2 eV uncertainty in the 5g - 4f X-ray.) Comparing the two model distributions in Table I, we see that the energy shifts are sensitive only to $\langle r^2 \rangle_{nuc}$ for these high angular momentum states. The result from Table II is $\Delta E^3_1 = -36$ eV for $\left[\langle r^2\rangle_{nuc}\right]^{\frac{1}{2}} = 5.5$ F. Thus the finite nuclear size caused a 10% increase in the third order VP contribution for $|k| = 1$. Since the $|k| \geqslant 2$ electrons are less sensitive to nuclear size, we estimate $-3 \text{ eV} \lesssim \Delta E^3_{k\geqslant 2}(R) \lesssim 0.9 \times \Delta E^3_{k\geqslant 2}(0) \cong -2.7$ eV. Thus the total contribution to the 5g - 4f X-ray from third order VP is $\Delta E^3 = -39$ eV as compared to the point nucleus value of -43 eV.

To solve for the energy shift to all orders, $\alpha(Z\alpha)^{n\geqslant 3}$, we construct the Green's function for the Dirac equation in the field of a finite size nucleus and remove the Uehling term. Since the third order calculation showed that the energy shift is sensitive only to $\langle r^2\rangle_{nuc}$,

a shell distribution (model I) is used with $R = 5.5$ F. The shell distribution is most convenient since both the internal and external wave functions are simple. The Green's function is then constructed[5] with the regular and irregular solutions of the Dirac equation: for $r < R$ these are spherical Bessel functions and for $r > R$ they are Whittaker functions. Both types of functions are subject to rapid, high precision numerical computation.[8] The Uehling contribution is obtained from the integral equation for the radial Green's function and may be expressed in terms of elementary and exponential integral functions. The details of these and of all other calculations mentioned in this letter will be given in a subsequent paper.

The results of the calculations are listed in Tables I and II. In the $R \to 0$ limit we get for orders $n \geqslant 3$, $\Delta E^{3+}_{k=1} = -46$ eV. From Eq. (3), the contribution of $|k| \geqslant 2$ to these orders is estimated to be -3 eV from third order and < 0.1 eV from orders $n \geqslant 5$. The total shift for orders $n \geqslant 3$ is then $\Delta E^{3+}(R=0) = -49$ eV in agreement with Ref. 6. For finite radius we rewrite Eq. (1)

$$\Delta E^{3+}(R) \cong \Delta E^{3+}_{k=1}(R) + \Delta E^{3+}_{k\geqslant 2}(0) , \tag{4}$$

where the $|k| \geqslant 2$ term is estimated from $\Delta E^{3+}_{1}(0)$ using Eq. (3). The accuracy of Eq. (4) is then estimated by

$$\begin{aligned} \delta &= \Delta E^{3+}_{k\geqslant 2}(R) - \Delta E^{3+}_{k\geqslant 2}(0) \\ &\cong 0.074 \times (\Delta E^{3}_{1}(R) - \Delta E^{3}_{1}(0)) + 0.008 \times (\Delta E^{5+}_{1}(R) - \Delta E^{5+}_{1}(0)) , \end{aligned} \tag{5}$$

where Eq. (3) has again been used. For the 5g - 4f transition, the

error in the approximation in Eq. (4) is then estimated to be less than 0.5 eV with the result that $\Delta E^{3+}(R) = -43$ eV. Thus, the finite nuclear size effect on VP increases the energy of the X-ray by 6 eV.

The VP densities ρ^3_1 and ρ^{3+}_1 calculated here with the energy contour along the imaginary axis satisfy gauge invariance. Therefore a good check on the numerical accuracy of these densities is provided by the evaluation of their integral over all space. It was found that for $r \lesssim 60$ F the densities were negative, while for $r \gtrsim 60$ F, they were positive; the densities were calculated out to $8\,\lambda\!\!\!^{-}_e$. The amount of charge contained in the region $r \lesssim 60$ F was $\sim -4 \times 10^{-3}\ |e|$, while the total charge out to $r = 8\,\lambda\!\!\!^{-}_e$ was $\sim -10^{-8}\ |e|$. Thus, better than five place accuracy was achieved for these densities.

To study the accuracy of the $m_e = 0$ and lowest order in R/r approximation[4] in the calculation of $\Delta\rho = \rho(R,r) - \rho(0,r)$, for $r \geqslant R$, we note that $\Delta\rho$ is proportional to the energy contour integral of the difference, ΔG, between the Green's function for the Dirac equation for a finite radius and point nucleus. The difference ΔG can be expressed as $\Delta G = f(R,z,m_e)\, W(r,z,m_e)$, where z is the energy, W involves products of Whittaker functions and f depends on R through the ratio of internal and external wave functions evaluated at R. The approximation of neglecting the electron mass in comparison to $1/a_0$ is implemented by setting $m_e = 0$ in both f and W. The approximation based on $R/a_0 \ll 1$ is obtained by expanding $f(R,z,m_e = 0)$ in powers of R and retaining only the first term. We have made calculations with and without these approximations. The

results for $|k| = 1$ are presented in Table III for the following three cases: (1) no approximation, (2) $m_e = 0$ only and (3) both $m_e = 0$ and lowest order in R/r. The results for the third case are in good agreement with Refs. 3 and 4. Numerically, the comment in Ref. 3 that corrections to $\Delta\rho(m_e=0)$ appear to $O((m_e r)^2)$ is supported by our results, and the functional form of $\Delta\rho\left(m_e=0, O(R/r)\right)$ is in good agreement with the analytic formula of Ref. 4. A simple comparison of $\Delta\rho$ in the various approximations is indicated by the values of the two integrals

$$\Delta Q_1 = \int_R^{30R} dr(4\pi r^2)\,\Delta\rho\,,$$

$$\Delta Q_2 = \int_{30R}^{\infty} dr(4\pi r^2)\,\Delta\rho\,, \qquad (6)$$

listed in Table III. The error commited in the $m_e = 0, O(R/r)$ approximation is seen to be 1 eV for the 5g - 4f transition and 13 eV for the 4f - 3d transition. To this error, the uncertainty in the $|k| = 1$ approximation, Eq. (5), must also be added. For such high angular momentum states, the accuracy of these approximations is nevertheless found to be quite adequate. The Uehling contribution was calculated in the two nuclear models and found to be the same for $\left[\langle r^2 \rangle_{nuc}\right]^{\frac{1}{2}} = 5.5$ F. When this contribution is subtracted from results of order $n \geq 1$, the $n \geq 3$ energy shifts are in agreement with Table I, as they must be.

The problem of vacuum polarization in superheavy electronic atoms, $Z \sim 170$, has also been investigated and will be reported elsewhere.

The author is very grateful to Dr. P. J. Mohr for many stimulating discussions on the theoretical and numerical aspects of this problem. Discussions with Dr. W. J. Swiatecki, Dr. E. Wichmann, Dr. R. N. Cahn, and Mr. L. D. McLerran are also gratefully acknowledged.

FOOTNOTES AND REFERENCES

* This work was supported by the U. S. Atomic Energy Commission.

1. M. S. Dixit, et al., Phys. Rev. Lett. 27, 878 (1971); H. K. Walter, et al., Phys. Lett. 40B, 197 (1972).
2. G. A. Rinker, Jr. and L. Wilets, Phys. Rev. Lett. 31, 1559 (1973).
3. J. Arafune, Phys. Rev. Lett. 32, 560 (1974).
4. L. S. Brown, Robert N. Cahn, and Larry D. McLerran, Phys. Rev. Lett. 32, 562 (1974).
5. E. H. Wichmann and N. M. Kroll, Phys. Rev. 101, 843 (1956).
6. J. Blomqvist, Nucl. Phys. B48, 95 (1972).
7. J. Heisenberg, et al., Phys. Rev. Lett. 23, 1402 (1969).
8. P. J. Mohr, Ph. D. Thesis, University of California, Berkeley, LBL-2011, May 14, 1973.

Table I. Absolute energy shifts (in eV) due to VP orders $(Z\alpha)^n$ in Pb using nuclear models I and II described in text. The $|k| \geqslant 1$ are calculated from Eqs. (4) and (5).

Order, $\|k\|$	Model R(F)	$5g_{9/2}$	$4f_{7/2}$	$3d_{5/2}$
$n = 3$, $\|k\| = 1$	I 5.5	43.39	79.24	151.9
	II 7.1	43.41	79.28	152.1
	I 0.6	45.16	85.10	177.0
	I 0.06	45.20	85.27	178.0
$n \geqslant 3$, $\|k\| = 1$	I 5.5	48.51	88.36	168.3
	I 0.6	51.34	97.12	202.6
	I 0.06	51.39	97.42	204.3
$n \geqslant 5$, $\|k\| = 1$	I 5.5	5.12	9.12	16.4
	I 0.06	6.19	12.15	26.3
$n \geqslant 3$, $\|k\| \geqslant 1$	I 5.5	51.9 ± 0.1	94.8 ± 0.5	181.7 ± 2

Table II. The VP contribution to $5g_{9/2} - 4f_{9/2}$ transition in Pb energy (in eV) for orders $(Z\alpha)^n$. The error in the contribution from $|k| \geqslant 2$ is less than 0.5 eV.

Order, $\|k\|$	$R_{rms} = 5.5$ F	$R = 0$
$n = 3$, $\|k\| = 1$	-36	-40
$\|k\| \geqslant 2$	- 3	- 3
$n \geqslant 5$, $\|k\| = 1$	- 4	- 6
$\|k\| \geqslant 2$	(< 0.1)	(< 0.1)
$n \geqslant 3$, $\|k\| \geqslant 1$	-43	-49

Table III. Perturbation of muonic levels (in eV) in Pb due to finite nuclear size effect on vacuum polarization, $|k| = 1$, orders $(Z\alpha)^n$. $\Delta Q_{1,2}$ are given by Eq. (6) in units of $-|e|$.

Order	Model	R(F)	Approx.	$5g_{9/2}$	$4f_{7/2}$	$3d_{5/2}$	ΔQ_1	ΔQ_2
$n \geq 1$	I	5.5	none	-5.48	-20.53	-116.1	7.020×10^{-2}	1.60×10^{-4}
			$m_e = 0$	-6.03	-21.43	-117.7	7.018×10^{-2}	1.95×10^{-4}
			$m_e = 0, O(R/r)$	-5.79	-19.99	-102.6	4.481×10^{-2}	1.91×10^{-4}
$n = 1$	I	5.5	none	-2.60	-11.46	- 80.02	6.598×10^{-2}	6.03×10^{-5}
	II	7.1	none	-2.60	-11.46	- 79.38		

0 0 0 0 4 2 0 4 1 8 1

CHAPTER II

VACUUM POLARIZATION IN HEAVY ION COLLISIONS

Submitted to Phys. Rev. Letters

0 0 0 0 4 2 0 4 1 8 2

VACUUM POLARIZATION IN HEAVY ION COLLISIONS*

Miklos Gyulassy

Lawrence Berkeley Laboratory
University of California
Berkeley, California 94720

July 10, 1974

ABSTRACT

The results of a study on vacuum polarization, orders $\alpha(Z\alpha)^n$, $n \geq 3$, for large Z systems encountered in heavy ion collisions are presented here. It is shown that the higher order vacuum polarization cannot prevent the $1S_{\frac{1}{2}}$ state from reaching the lower continuum, $E = -m_e c^2$, for some critical charge $Z_{cr} \sim 170$. In addition, the stability and localization of a helium-like system for $Z > Z_{cr}$ is demonstrated.

An interesting application of heavy ion collisions is to the study of quantum electrodynamics of strong fields. For short times, at least, systems with large effective charge Z will be formed with $Z\alpha > 1$. In the strong fields of such systems, highly relativistic electronic bound states are expected to occur with binding energies B exceeding the electron rest mass m_e, and for some critical charge, $Z_{cr} \sim 170$, the $1S_{\frac{1}{2}}$ state is expected to reach the lower continuum with $B = 2m_e$.[1] For $Z > Z_{cr}$, it has been predicted[2,3] that spontaneous e^+e^- pair production will occur with the subsequent capture of two electrons into a tightly bound helium-like state and the ejection of two positrons into continuum states. These predictions

have been based on solutions of the Dirac equation for finite size nuclei in which radiative corrections such as vacuum polarization (VP) and the Lamb shift are ignored. For these predictions to be applicable to heavy ion collisions, it is essential to show that radiative corrections are indeed negligible for large $Z \sim Z_{cr}$ and thus cannot prevent the $1S_{\frac{1}{2}}$ state from reaching the lower continuum. Several qualitative arguments[2,3] and a model calculation based on effective limiting field Lagrangians[4] suggest that the effect of VP does remain small up to Z_{cr}. Yet, a complete quantum electrodynamic calculation had not been carried out to all orders in $Z\alpha$. The purpose of this Letter, then, is to present the results of a numerical calculation of the higher order VP, orders $\alpha(Z\alpha)^n$, $n \geq 3$, based on the methods of Wichmann and Kroll.[5] The results confirm that VP remains a small perturbation even up to Z_{cr}.

Although the effect of higher order VP is always much less than that of the first order (Uehling) potential in atoms with $Z \leq 100$, the results of Wichmann and Kroll[5] for a point nucleus show that the size of the higher order VP increases sharply near $Z\alpha = 1$. If the VP charge accumulated at the origin for orders $\alpha(Z\alpha)^n$, $n \geq 3$, is denoted by Q_{WK}^{3+}, then while Q_{WK}^{3+} is finite and much smaller than the nuclear charge when $Z\alpha = 1$ ($|Q_{WK}^{3+}| \approx 0.05|e| << 137|e|$), $dQ_{WK}^{3+}/dZ = -\infty$ at $Z\alpha = 1$. Furthermore, the infinite slope of Q_{WK}^{3+} can be seen to come from the lowest angular momentum $\left(k = \pm(j + \frac{1}{2}) = \pm 1\right)$ contribution to the VP density. The higher angular momentum ($|k| \geq 2$) contribution to Q_{WK}^{3+} is seen to vary smoothly past $Z\alpha = 1$ until $Z\alpha = 2$, where the $|k| = 2$ contribution becomes singular. Of course, these singularities in the VP charge density arise because of the assumed point structure of the

nucleus. Nevertheless, these results indicate that we may expect a rapid increase in the higher order VP for $Z\alpha > 1$ when the finite size of the nucleus is taken into account. Furthermore, the fastest growing part should be that due to the lowest angular momentum ($|k| = 1$) electron loops. Another important property that can be deduced from the results of Ref. 5 is the relative size of the $|k| = 1$ to the $|k| \geq 2$ contributions to the VP charge density. The $|k| \geq 2$ contribution was found to be always less than 10% of the $|k| = 1$ contribution for orders $\alpha(Z\alpha)^n$, $n \geq 3$, for all $Z\alpha \leq 1$.[6,7] Therefore, a good approximation in the calculation of higher order VP, relevant for heavy ion collisions, is obtained by calculating the $|k| = 1$ contribution exactly for finite size nuclei while neglecting the $|k| \geq 2$ contribution. In this way the dominant and fastest growing part of the VP density is calculated exactly while leaving an overall uncertainty of less than 10% in the final results due to neglect of the $|k| \geq 2$ contribution.

The calculation of the VP density, ρ_{VP}, involves an energy contour integral of the trace of the Green's function, TrG, for the Dirac equation.[5] For $Z < Z_{cr}$, the choice of this contour is clear and is given by C_0 in Fig. 1. With this contour, ρ_{VP} is equal to the vacuum expectation value of the Heisenberg current operator, $\langle 0|J_0(x)|0\rangle$. Thus to first order in α and to all orders in $Z\alpha$, ρ_{VP} can be written formally as

$$\rho_{VP} = \frac{|e|}{2}\left\{\sum_{+} \psi_{+}^{2} - \sum_{-} \psi_{-}^{2}\right\} , \qquad (1)$$

where $\psi_{\pm}$ refer to the positive and negative energy eigenfunctions of the Dirac equation.[8] Here positive energy refers to all eigenvalues

greater than $-m_e$. In particular, the $1S_{\frac{1}{2}}$ state is contained in the first sum. The helium-like charge density, ρ_{He}, is defined as the expectation value of the current operator for a state of two electrons in the $1S_{\frac{1}{2}}$ state: $\langle 2e^-(1S)|J_0(x)|2e^-(1S)\rangle$. This density is related to ρ_{VP} by

$$\rho_{He} = -2|e|\psi^2_{1S_{\frac{1}{2}}} + \rho_{VP} \quad , \tag{2}$$

which is equivalent to the addition of a counter-clockwise contour around the 1S pole to C_0 in Fig. 1. The sum of these contours may then be deformed to C_{He}. For $Z < Z_{cr}$, then, ρ_{VP} and ρ_{He} are computed via a contour integral along paths C_0 and C_{He} respectively (in units of $|e|$).

For $Z > Z_{cr}$, the $1S_{\frac{1}{2}}$ pole moves off the physical sheet through the branch point of the lower continuum. Since the vacuum around the bare nucleus can then decay into a helium-like state plus two free positrons,[2,3] it is natural to redefine the vacuum to correspond to the helium-like state.[9] The VP density, ρ_{VP}, is thus defined to equal ρ_{He} for $Z > Z_{cr}$. While Eq. (2) is no longer meaningful for $Z > Z_{cr}$, the contour integral representation for ρ_{He} around path C_{He} in Fig. 1 is still well defined. The charge distribution of the overcritical vacuum is thus calculated with contour C_{He}.

The higher order VP density, ρ^{3+}, for $k = \pm 1$ and $Z < Z_{cr}$ is calculated by expanding TrG in terms of radial Green's functions, TrG_k, and removing the first order Green's functions, TrG_k^1. Isolating the terms corresponding to $k = \pm 1$, the contour integral over path C_0 is performed. In practice, C_0 is deformed to the imaginary axis I, picking up the negative of the residues of all poles of $TrG_{k=\pm 1}$ which lie between zero and $-m_e$. The negative of

those residues are, of course, the modulus squared of the normalized bound state wavefunctions. The calculation of ρ_{He} involves adding to the contour integral along I all but the $1S_{\frac{1}{2}}$ wave functions squared with $m_e < B < 2m_e$.

In addition to ρ^{3+}, the third order, $\alpha(Z\alpha)^3$, VP density, ρ^3, is calculated for $k = \pm 1$ and $Z < Z_{cr}$ to provide a check on internal consistency and to estimate the dependence of ρ^{3+} on different nuclear charge densities. The calculation of ρ^3 involves the contour integral of the third order Green's function, $TrG_k{}^3$, for $k = \pm 1$ along contour I. Two models for the nuclear charge densities were used for calculating ρ^3: (I) a shell density, $\rho_{Nuc} = \delta(r - R)/4\pi R^2$ and (II) a uniform density, $\rho_{Nuc} = \theta(R - r)/(4\pi R^3/3)$. The nuclear radius was chosen to be 10 fm in both models. The densities ρ^{3+} and ρ_{He} were calculated with model I.

The construction of TrG_k, $TrG_k{}^1$, and $TrG_k{}^3$ is the same here as in Ref. 6 and will be discussed in more detail in a subsequent paper.

The following tests check the numerical accuracy of the constructed Green's functions. First, the location of the $1S_{\frac{1}{2}}$ and $2P_{\frac{1}{2}}$ poles were computed as a function of Z. The values of $(Z\alpha)_{cr}$ were determined for model I nuclei for R = 8, 10, and 12 fm, with $(Z\alpha)_{cr} = 1.25189$, 1.27459, and 1.29530 respectively for the $1S_{\frac{1}{2}}$ state, and $(Z\alpha)_{cr} = 1.383$ for R = 10 fm, for the $2P_{\frac{1}{2}}$ state, in agreement with Ref. 3. Furthermore, in agreement with Ref. 2, dB/dZ at $Z = Z_{cr}$ was calculated to be 27 keV for the $1S_{\frac{1}{2}}$ state and 35 keV for the $2P_{\frac{1}{2}}$ state. Secondly, the residues at those poles were calculated in order to check that the normalized bound state wave functions were given correctly. All $S_{\frac{1}{2}}$ and $P_{\frac{1}{2}}$ wavefunctions

calculated thereby were normalized to unity to better than one part per 10^5. The $R \to 0$ limit was taken numerically for $Z\alpha < 1$ to check that these wavefunctions reduce to the point nucleus form. In addition, the $\langle 1/r \rangle$ was computed for these wavefunctions since $dB/dZ \approx \alpha m_e c^2 \langle 1/r \rangle$ which can be compared to the values computed above; at $Z = Z_{cr}$, e.g., $dB/dZ = 28$ keV and 37 keV for the $1S_{\frac{1}{2}}$ and $2P_{\frac{1}{2}}$ states respectively, in good agreement with the above values. Thirdly, for the special case of $Z = 82$, extensive checks on the charge densities were made showing that the limit $R \to 0$ and the finite nuclear size effect agreed with other calculations.[6] Finally, the total space integral Q_{He} of ρ_{He} was computed for the range $0.6 \leq Z\alpha \leq 1.38$ since the extent to which $Q_{He} = -2|e|$ measures the accuracy of the numerical contour integration along I. The computed values of Q_{He} were equal to $-2|e|$ to better than 1 part per 10^4 over the entire range. The accuracy of the computed ρ^{3+} for $Z < Z_{cr}$ is less due to cancellations necessary to insure that the total charge of the vacuum vanish. This accuracy is estimated from the magnitude of the ratio of the integral of ρ^{3+} over all space $(r \lesssim 13\lambda\!\!\!^{-}_e)$ to the integral over the range where ρ^{3+} is negative $(r \lesssim 100$ fm). This ratio was found to be $\lesssim 0.01$, indicating a numerical accuracy on the order of one percent.

The computed $1S_{\frac{1}{2}}$ energy shifts for $Z < Z_{cr}$ due to higher order VP are listed in Table I. These energy shifts should be compared to the shift due to the Uehling potential. The Uehling potential is attractive and increases the binding energy of the $1S_{\frac{1}{2}}$ state by approximately 10 keV at Z_{cr}.[1,10] The higher order VP is repulsive but is seen in Table I to reduce the binding energy by only 1 keV at Z_{cr}.

The last two lines, in particular, in Table I indicate the absence of any singularities of ΔE^{3+} at Z_{cr}. Thus, even though the shift ΔE^{3+} due to higher order VP increases rapidly for $Z\alpha > 1$, it remains too small to prevent the $1S_{\frac{1}{2}}$ state from reaching the lower continuum. Furthermore, the results for third order indicate that the dependence of ΔE^{3+} on the specific nuclear charge density is a 10% effect, i.e., on the same order as the uncertainty in ΔE^{3+} due to neglect of the $|k| \geq 2$ contribution to the VP density.

Since the results for $Z < Z_{cr}$ show that VP remains a small perturbation up to Z_{cr}, the use of the unperturbed Green's function, $\mathrm{Tr}G_k$ and $\mathrm{Tr}G_k^{1}$, in computing $\rho^{3+} \equiv \rho_{He}$ for $Z > Z_{cr}$ will not lead to large errors. In Fig. 2(a), ρ_{He} is plotted for several values of $Z\alpha$ around $(Z\alpha)_{cr} = 1.27459$. The continuity of ρ_{He} at Z_{cr} was examined by calculating ρ_{He} for $Z\alpha = 1.2732, 1.27445, 1.27545,$ and 1.28 and checking point by point in the range $0 \leq r \lesssim 13\lambda\!\!\!^{-}_e$ that the values of ρ_{He} for the different Z can be smoothly connected. The increased localization and continuity of ρ_{He} as a function of Z is illustrated in Fig. 2(b), where the average $\langle 1/r \rangle$ for ρ_{He} is plotted. These results demonstrate that the helium-like system is stable and well behaved around Z_{cr} and that the charge density of the overcritical vacuum is indeed highly localized.[11]

It should be noted that for $Z\alpha = 1.383$, the $2P_{\frac{1}{2}}$ state reaches the lower continuum and the helium-like system will decay to a beryllium-like system plus two free positrons.[2,3] The charge density of the beryllium-like system can be studied in the same way as ρ_{He}, simply by shifting the contour C_{He} to the right of the $2P_{\frac{1}{2}}$ pole.

In this Letter the effect of VP in very high Z atoms has been considered. The effect of the Lamb shift has been estimated by other workers,[10] but agreement on the size of that effect has not yet been reached. More work is needed on that problem.

The author gratefully acknowledges helpful conversations with Dr. P. J. Mohr, Dr. W. Greiner, Dr. W. J. Swiatecki, and Dr. E. H. Wichmann.

FOOTNOTES AND REFERENCES

* This work was supported by the U. S. Atomic Energy Commission.

1. W. Pieper and W. Greiner, Z. Physik 218, 327 (1969).
2. B. Muller, J. Rafelski, and W. Greiner, Z. Physik 257, 62 (1972) and Z. Physik 257, 183 (1972).
3. Ya. B. Zel'Dovich and V. S. Popov, Sov. Phys.-Usp. 14, 673 (1972).
4. J. Rafelski, W. Greiner, and L. P. Fulcher, Nuovo Cimento 13, 135 (1973).
5. E. H. Wichmann and N. M. Kroll, Phys. Rev. 101, 843 (1956).
6. M. Gyulassy, Phys. Rev. Letters 32, 1393 (1974).
7. L. S. Brown, R. N. Cahn, and L. D. McLerran, University of Washington preprint, RLO-1388-677 (1974).
8. See, e.g., Ref. 3, p. 687.
9. L. Fulcher and A. Klein, Phys. Rev. D8, 2455 (1973); J. Rafelski, B. Muller, and W. Greiner, Nucl. Phys. B68, 585 (1974).
10. G. Soff, B. Muller, and J. Rafelski, University of Pennsylvania preprint, UPR-0033N (1974).
11. These points have also been discussed by Rafelski et al. (9) using different methods.

Table I. The $1S_{\frac{1}{2}}$ energy shifts in eV due to vacuum polarization orders $\alpha(Z\alpha)^n$, with ΔE^{3+} for $n \geq 3$, and $\Delta E^3_{I,II}$ for $n = 3$, model I and II nuclei. $E_{1S\frac{1}{2}}$ and $E_{2P\frac{1}{2}}$ locate the bound state poles in units of m_e. The nuclear charge density for all but the last column was taken to be model I with $R = 10$ fm.

Z	$E_{1S\frac{1}{2}}$	$E_{2P\frac{1}{2}}$	ΔE^{3+}	$\Delta E_I{}^3$	$\Delta E_{II}{}^3$
0.95	0.362	0.817	6.26×10	4.70×10	4.92×10
1.12	0.137	0.570	3.07×10^2	1.97×10^2	2.11×10^2
1.205	-0.550	0.265	6.41×10^2	3.68×10^2	3.99×10^2
1.2732	-0.990	-0.118	1.14×10^3	5.66×10^2	6.20×10^2
1.27445	-0.999	-0.126	1.15×10^3	5.70×10^2	6.24×10^2

FIGURE CAPTIONS

Fig. 1. Singularities of the Green's function in the complex energy plane and contours C_0, C_{He}, and I giving the VP and helium-like charge densities in units of $|e|$.

Fig. 2. (a) The helium-like charge density for several values of $\gamma \equiv Z\alpha$ around $(Z\alpha)_{cr} = 1.27459$ with a model I, R = 10 fm nucleus.

(b) The average $\langle 1/r \rangle$ for ρ_{He} as a function of $Z\alpha$.

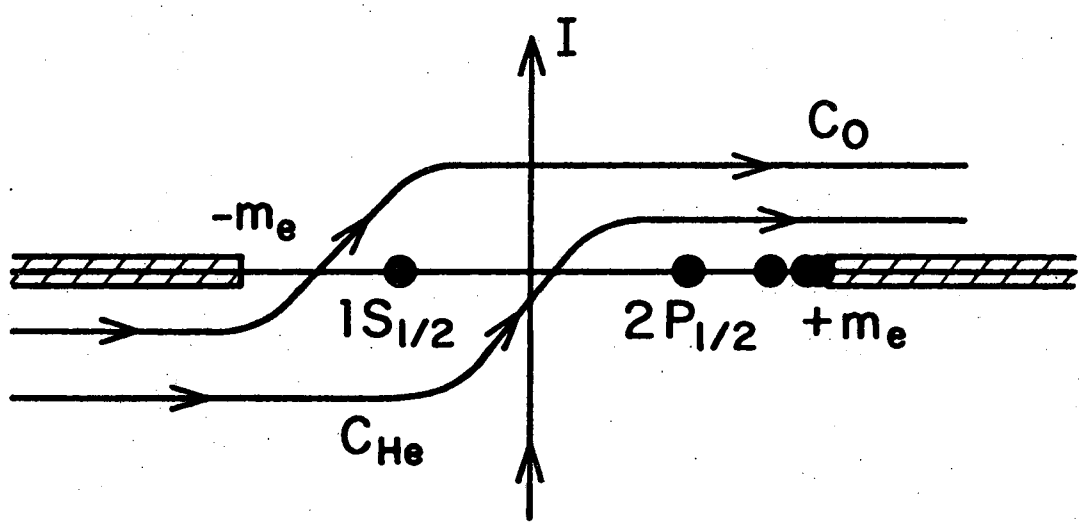

XBL 747-3588

Fig. 1.

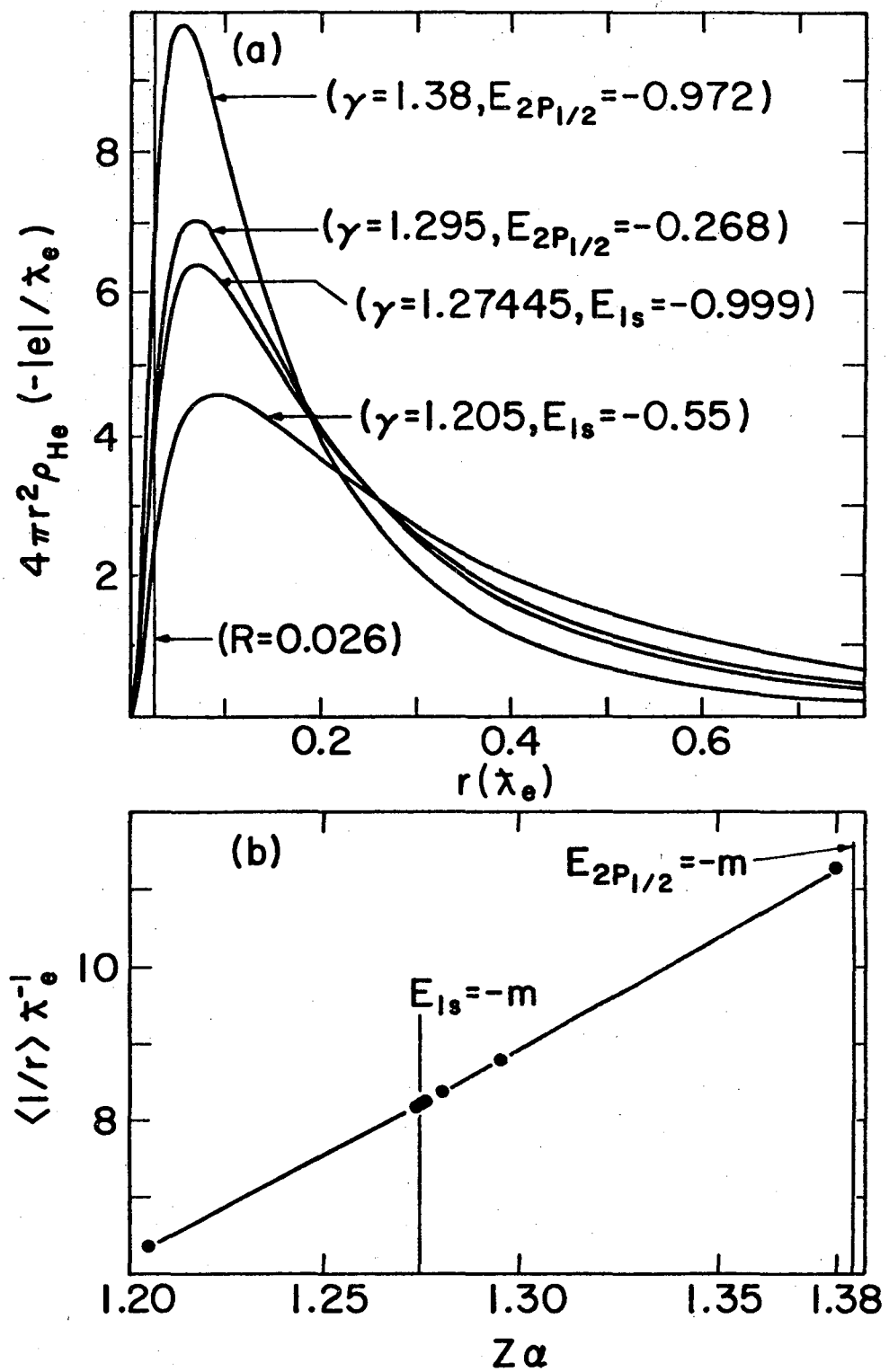
(a)
(γ=1.38, E2P1/2=-0.972)
(γ=1.295, E2P1/2=-0.268)
(γ=1.27445, E1s=-0.999)
(γ=1.205, E1s=-0.55)
(R=0.026)
4πr²ρHe (-|e|/λ̄e)
r(λ̄e)
(b)
E2P1/2=-m
E1s=-m
⟨1/r⟩ λ̄e⁻¹
Zα
XBL 747-3589

Fig. 2.

0 0 0 0 4 2 0 4 1 8 8

CHAPTER III

HIGHER ORDER VACUUM POLARIZATION FOR FINITE RADIUS NUCLEI

Submitted to Nucl. Phys. B

HIGHER ORDER VACUUM POLARIZATION FOR FINITE RADIUS NUCLEI*

Miklos Gyulassy

Lawrence Berkeley Laboratory
University of California
Berkeley, California 94720

September 17, 1974

ABSTRACT

The calculation of the higher order, $\alpha(Z\alpha)^n$, $n \geq 3$, vacuum polarization charge density induced by high Z nuclei of finite extent is discussed here. The Wichmann-Kroll formalism relating the vacuum polarization charge density to the Green's function of the Dirac equation is reviewed with attention drawn to modifications necessary for very large Z systems $(Z > 137)$ encountered in heavy ion collisions. This paper is concerned with the construction of the radial Green's functions for the Dirac equation in the field of finite radius nuclei and on the numerical calculation of the higher order vacuum polarization density from those Green's functions. Specific calculations are made for muonic Pb and superheavy electronic atoms. The results from these calculations have been published elsewhere but are further elaborated upon here.

* This work was supported by the U. S. Atomic Energy Commission.

1. Introduction and Summary

The purpose of this paper is to supplement the discussion of two previous papers (1,2) on the calculation of the higher order vacuum polarization charge density in the field of high Z nuclei of finite extent. The problem considered in Ref. (1) was the calculation of the nuclear size corrections to the vacuum polarization (VP) density for orders $\alpha(Z\alpha)^n$, $n \geq 3$, in muonic Pb. In particular, the effect of those corrections on the $5g_{9/2}$-$4f_{7/2}$ transition was calculated. This is of interest in view of the 42 ± 20 eV discrepancy reported between theory and experiment (3-5). As reported in Ref. (1), these corrections do increase the discrepancy but by only 6 eV. In the work of Arafune (4) and Brown et al. (5) approximations based on the smallness of the electron mass and of the nuclear radius were made. The accuracy of those approximations was studied in Ref. (1) and found to be quite adequate (~1 eV) for this transition in muonic Pb. In Ref. (2), the effect of the higher order VP density on electronic bound states in the field of very large Z nuclei was discussed. The main conclusion reported there was that the higher order VP cannot prevent the $1S_{1/2}$ state from reaching the lower continuum ($E_{1S_{1/2}} = -m_e$) for some critical value of the nuclear charge $Z_{cr} \sim 170$, (6). Then the calculation of the VP charge density for overcritical fields (7) was discussed, and finally, the stability and localization of the helium-like charge density ρ_{He} for Z in the neighborhood of Z_{cr} were demonstrated through precise calculations of ρ_{He} for $Z < Z_{cr}$ and $Z > Z_{cr}$. In this paper, we discuss the details and methods used in arriving at the results reported in Refs. (1,2). This paper, then, serves as the basis for both those papers.

The discussion here is divided into the following sections. In section 2, the Wichmann-Kroll formalism (8) for the calculation of the VP density ρ_{VP} is reviewed. The modifications necessary for very large Z nuclei are discussed in detail, and formal relations between ρ_{VP} and the Green's function for the Dirac equation are established. A partial wave decomposition of ρ_{VP} is then made, and each partial wave contribution is further expanded in powers of the coupling constant $Z\alpha$. Then, the regularization of the formal expressions involving the Green's functions is discussed and illustrated through a calculation of ρ_{VP} in the field of a constant external potential.

In section 3, expressions for the radial Green's functions, required in the calculation of the partial wave contributions to ρ_{VP}, are constructed valid to all orders in $Z\alpha$. The construction of the radial Green's functions to first and third order in $Z\alpha$ is then carried out in section 4.

Section 5 is designed to supplement the discussion of Ref. (1). While the emphasis in Ref. (1) was on the energy shifts due to nuclear size corrections to ρ_{VP}, the emphasis in section 5 is on the effect of those corrections on ρ_{VP} itself. The results for high Z systems reported in Ref. (2) are further elaborated upon in section 6. The critical charge Z_{cr} is calculated for the particular model of the nuclear charge density considered in Ref. (2). The $1S_{1/2}$ wavefunctions and the higher order VP density for $137 < Z < Z_{cr}$ are also calculated. Again, the emphasis is on the structure of ρ_{VP} rather than the resulting energy shifts. In both sections 5 and 6, ρ_{VP} is calculated only for the lowest partial wave $(j = 1/2)$ contribution. The contribution from higher partial waves $(j \geq 3/2)$

may be estimated from the results of a point nucleus as in Refs. (1,2).

Finally, in section 7, the numerical techniques applied to the evaluation of the special functions and integrations in the calculation of ρ_{VP} are discussed.

2. Relation of ρ_{VP} to the Green's function of the Dirac equation

A. Formal Expressions

The VP density ρ_{VP} is given by the vacuum expectation value of the $\mu = 0$ component of the current operator,*

$$J_\mu(x) = -\frac{|e|}{2}\left[\bar{\psi}(x),\gamma_\mu\psi(x)\right] \quad . \tag{2.1}$$

In terms of the Feynman propagator $S_F(x,x')$, ρ_{VP} can be written (10) as

$$\rho_{VP} = i|e|\mathrm{Tr}\left(S_F(x,x')\gamma_0\right)\Big|_{x'\to x} \quad , \tag{2.2}$$

where S_F satisfies

$$\left(\gamma^\mu\left(i\partial_\mu - e\,A_\mu(x)\right) - m_e\right) S_F(x,x') = \delta^4(x - x') \quad . \tag{2.3}$$

For time independent potentials A_μ, $S_F(x,x')$ depends on time only through $t - t'$, and consequently,

$$i\,S_F(\underset{\sim}{x},\underset{\sim}{x}';\, t - t')\gamma_0 = \frac{1}{2\pi i}\int_C dz\, e^{-i(t-t')z}\, G(\underset{\sim}{x},\underset{\sim}{x}';\, z), \tag{2.4}$$

where the Green's function G then satisfies

---

* The metric, gamma matrices, units ($\hbar = c = 1$), and notation are chosen to agree with the conventions of Ref. (9).

$$\left(\underset{\sim}{\alpha}\cdot\left(-i\underset{\sim}{\nabla} - e\underset{\sim}{A}(\underset{\sim}{x})\right) - z + eA_0(\underset{\sim}{x}) + \beta m_e\right) G(\underset{\sim}{x},\underset{\sim}{x}';\ z) = \delta^3(\underset{\sim}{x} - \underset{\sim}{x}') \quad , \tag{2.5}$$

and the contour C is determined from the Feynman boundary conditions (which depend on the definition of the vacuum).

In terms of G, eq. (2.2) can be written as

$$\rho_{VP} = \frac{|e|}{2\pi i} \int_C dz\ \mathrm{Tr}\ G(\underset{\sim}{x},\underset{\sim}{x}';\ z)\Big|_{\underset{\sim}{x}'\to\underset{\sim}{x}} \quad . \tag{2.6}$$

This relation, then, is the basis of the Wichmann-Kroll formalism (8) for the calculation of ρ_{VP} to all orders in $Z\alpha$. Note that the Green's function in this relation must be properly regulated to insure that the limit $\underset{\sim}{x}' \to \underset{\sim}{x}$ exists and that the integral over z converges. This regularization is discussed in the next section. In this section, though, all expressions are to be understood to involve only regulated Green's functions.

The well-known formal solution of eq. (2.5),

$$G(\underset{\sim}{x},\underset{\sim}{x}';\ z) = \sum_E \frac{\psi_E(\underset{\sim}{x})\ \psi_E^\dagger(\underset{\sim}{x}')}{E - z} \quad , \tag{2.7}$$

where ψ_E are properly normalized eigenfunctions of the Dirac equation, exhibits the singularities of G in the complex z-plane. These singularities are illustrated in Fig. 1.

The path of the contour C in eq. (2.6) through these singularities is chosen so that the contour lies above the singularities of G associated with positive energy states and below the singularities associated with negative energy states. With this choice of C, S_F in eq. (2.4) satisfies the Feynman boundary conditions. The definition of which states correspond to positive and negative energy states is

equivalent to the definition of the vacuum and is completely determined by the energy E_C, where the contour crosses the real axis in Fig. 1. When there is no external potential, E_C can obviously be chosen anywhere between $E = \pm m_e$. As the strength of the potential increases, bound states are formed and G develops poles between the two branch points at $E = \pm m_e$. The energy E_C must then be adjusted so that all bound state energies remain greater than E_C for the case of attractive potentials or less than E_C for the case of repulsive potentials. With this specification of E_C, the conventional vacuum in the bound-interaction (Furry) picture is obtained (11). On the other hand, if E_C is chosen so that there are bound states with energies both greater and less than E_C, then the corresponding vacuum state will be charged. This is easily seen by calculating ρ_{VP} in eq. (2.6) with two different contours corresponding to different choices of E_C. Figure 1 illustrates two such contours.

The contour C_0 corresponds to the usual definition of the vacuum for the case of attractive potentials since all bound state energies are greater than E_C. On the other hand, C_{He} corresponds to a charged vacuum (2) since, from eq. (2.7), the difference of the VP densities calculated in eq. (2.6) with contours C_0 and C_{He} is just $2|e||\psi_{1S_{1/2}}(x)|^2$. Thus, in fact, eq. (2.6) with $C = C_{He}$ gives a helium-like charge density ρ_{He} that contains a total charge of $-2|e|$.

In the choice of the contour C_0 for the calculation of ρ_{VP}, it was assumed that all binding energies were less than $2m_e$ and, thus, that no poles of G have crossed from one branch point to the other. However, for overcritical fields $(Z > Z_{cr})$ the pole of G

corresponding to the $1S_{1/2}$ state (the $1S_{1/2}$ pole) moves from the branch point at $E = +m_e$ through the branch point at $E = -m_e$ off of the "physical" sheet of the Riemann surface for the Green's function. In that case, the vacuum is predicted to decay spontaneously into a helium-like state* plus two free positrons (7). Thus, the stable VP density for $Z > Z_{cr}$ corresponds to a helium-like density ρ_{He} obtained with contour C_{He} in eq. (2.6) rather than to the analytic continuation of ρ_{VP} from $Z < Z_{cr}$, (2). Furthermore, if the potential becomes so strong that the $2P_{1/2}$ pole also moves off the physical sheet through the branch point at $E = -m_e$, then the helium-like state will spontaneously decay to a berylium-like state plus two more positrons, and consequently, the stable vacuum must again be redefined by shifting the contour C_{He} to the right of the $2P_{1/2}$ pole. Each time a bound state pole moves off the physical sheet, the contour in eq. (2.6) must be shifted so that E_C stays to the right of the branch point at $-m_e$ and to the left of any remaining bound state poles on the physical sheet. A simple expression for the stable vacuum density for any strength of the potential can be written by deforming the contour C to the imaginary axis I. Thus, from eq. (2.7),

$$\rho_{VP} = |e| \left\{ \sum_{-m_e<E<0} |\psi_E(\underset{\sim}{x})|^2 + \frac{1}{2\pi} \int_{-\infty}^{\infty} dy \; \mathrm{Tr}\; G(\underset{\sim}{x},\underset{\sim}{x}';\, iy)\Big|_{\underset{\sim}{x}'\to\underset{\sim}{x}} \right\}. \tag{2.8}$$

---

* We neglect interaction between the two electrons.

This equation contains the fact that each time a pole of G moves off the physical sheet through the branch point at $-m_e$, the total charge of the vacuum around the nucleus changes by $-2|e|$.*

For spherically symmetric potentials, the Green's function $G(\underset{\sim}{x},\underset{\sim}{x}';\ z)$ has a partial wave decomposition (12) in terms of radial Green's functions G_k satisfying

$$\begin{bmatrix} m_e + V(r) - z & -\frac{1}{r}\frac{d}{dr}r + \frac{k}{r} \\ \frac{1}{r}\frac{d}{dr}r + \frac{k}{r} & -m_e + V(r) - z \end{bmatrix} G_k(r,r';\ z) = \frac{\delta(r-r')}{rr'}, \tag{2.9}$$

where $k = \pm(j + 1/2)$ for a given total angular momentum j. From the following relation (8,12)

$$\mathrm{Tr}\ G(\underset{\sim}{x},\underset{\sim}{x}';\ z)\Big|_{\underset{\sim}{x}'\to\underset{\sim}{x}} = \sum_k \frac{2|k|}{4\pi}\ \mathrm{Tr}\ G_k(|\underset{\sim}{x}|,|\underset{\sim}{x}'|;\ z)\Big|_{\underset{\sim}{x}'\to\underset{\sim}{x}}, \tag{2.10}$$

the contribution to the VP density for a given k is then given by

$$\begin{aligned}\rho_k(r) &= \frac{|e||k|}{(2\pi)^2 i}\int_C dz\ \mathrm{Tr}\ G_k(r,r';\ z)\Big|_{r'\to r} \\ &= \frac{|e||k|}{2\pi}\left\{\sum_{-m_e<E<0} |\psi_{E,k}(r)|^2 + \frac{1}{2\pi}\int_{-\infty}^{\infty} dy\ \mathrm{Tr}G_k(r,r';iy)\Big|_{r'\to r}\right\},\end{aligned} \tag{2.11}$$

---

* $+2|e|$ amount of charge escapes with two free positrons; $-2|e|$ is localized with two bound electrons.

where $\psi_{E,k}$ are the normalized radial wave functions with eigenvalues E and k for the potential V.

For a given angular momentum j, there exists a simple symmetry for G_k. Let $G_k(V;\, r,r';\, z)$ be the solution of eq. (2.9). Then it is easily seen that

$$G_{-k}(V;\, r,r';\, z) = -\sigma_1\, G_k(-V;\, r,r';\, -z)\, \sigma_1 \quad , \tag{2.12}$$

where $\sigma_1 = \begin{pmatrix} 0 & 1 \\ 1 & 0 \end{pmatrix}$. Thus,

$$\mathrm{Tr}\, G_{-k}(V;\, r,r';\, z) = -\,\mathrm{Tr}\, G_k(-V;\, r,r';\, -z) \quad . \tag{2.13}$$

With this relation, the sum of the VP densities for $k = \pm|k|$, $\rho_{|k|} = \rho_k + \rho_{-k}$, can be written as

$$\rho_{|k|} = \frac{|e||k|}{2\pi} \left\{ \sum_{k=\pm|k|} \sum_{-m_e<E<0} |\psi_{E,k}(r)|^2 \right.$$

$$\left. + \frac{1}{2\pi} \int_{-\infty}^{\infty} dy\, \mathrm{Tr}\Big(G_k(V;\, r,r';\, iy) - G_k(-V;\, r,r';\, iy)\Big)\Big|_{r'\to r} \right\} . \tag{2.14}$$

The integral along the imaginary axis is manifestly odd as a function of V. To see that the sign of the first term also changes as $V \to -V$, note that for repulsive potentials the bound state poles emerge from the branch point at $-m_e$ and approach the branch point at $+m_e$ from the left. The contour C giving the VP density in eq. (2.11) must then cross the real axis to the right of those poles on the physical sheet but to the left of the branch point at $+m_e$. Deforming C to the imaginary axis I, the residues of $\mathrm{Tr}\, G_k$, $k = \pm|k|$, in the

interval $0 < E < m_e$ must then be added to the contour integral along I with the opposite sign as in eq. (2.14). Thus $\rho_{|k|}(r)$ is an odd function of V as required by Furry's theorem.

In addition to a partial wave expansion of ρ_{VP}, it is useful to consider the expansion of each ρ_k in powers of the external potential. Writing this potential as $V = -Z\alpha\, V_0(r)$, where $Z\alpha$ is an expansion parameter and V_0 is a function of r, the power series expansion in $Z\alpha$ for the Green's function is given by the Neumann series for the resolvent

$$G_k = \sum (Z\alpha)^n\, G_k^{\,n} = \sum (Z\alpha)^n\, G_k^{\,0}(V_0\, G_k^{\,0})^n \quad , \tag{2.15}$$

where $G_k^{\,0}$ is the resolvent in the absence of an external potential. The trace of the nth order Green's function for a given k is then given by

$$\mathrm{Tr}\, G_k^{\,n}(r,r') = \int_0^\infty \prod_{i=1}^{n} \left(dr_i\, r_i^{\,2}\, V_0(r_i)\right)$$

$$\times\, \mathrm{Tr}\left(G_k^{\,0}(r,r_1)\cdots G_k^{\,0}(r_n,r')\right) \quad . \tag{2.16}$$

The nth order VP charge density for $k = \pm|k|$ is thus given by

$$\rho^n_{|k|}(r) = \frac{|e||k|}{(2\pi)^2 i}(Z\alpha)^n \int_C dz\, \mathrm{Tr}\left(G_k^{\,n}(r,r';\, z) + G_{-k}^{\,n}(r,r';\, z)\right)\Big|_{r'\to r} . \tag{2.17}$$

From eqs. (2.13 and 2.16) ,

$$\mathrm{Tr}\, G_{-k}^{\,n}(r,r';\, z) = -(-1)^n\, \mathrm{Tr}\, G_k^{\,n}(r,r';\, -z) \quad . \tag{2.18}$$

Also for a given n and k, $\mathrm{Tr}\, G_k^{\,n}$ has no poles between $\pm m_e$. Therefore, deforming C to the imaginary axis, $\rho^n_{|k|}$ can be written as,

$$\rho^n_{|k|}(r) = \begin{cases} \dfrac{|e|\,|k|}{(2\pi)^2}\, 2(Z\alpha)^n \displaystyle\int_{-\infty}^{\infty} dy\ \mathrm{Tr}\, G_k^{\,n}(r,r';\, iy)\Big|_{r'\to r} & (n \ \text{odd}) \\ 0 \qquad (n \ \text{even}) \end{cases} \tag{2.19}$$

This equation again contains the requirement of Furry's theorem that the VP density must be an odd function of Z.

B. Regularization

The formal manipulations that led to the equations of the previous section are of course justified only if the operations indicated in them, such as taking limits and performing integrations, are well defined and if there is no ambiguity associated with the interchange of those operations. However, as noted in the previous section, eq. (2.6) is not well defined since neither the limit $\underset{\sim}{x}' \to \underset{\sim}{x}$ nor the integral over z exist. Therefore a regulator scheme is essential if meaningful results are to be obtained from any of the equations of the previous section.

One well-known regulator scheme that is known to give unambiguous, gauge invariant results is due to Pauli and Villars [14]. In that scheme the Green's function is regulated with auxiliary masses as follows: let $G(m_i)$ denote the solution of eq. (2.5) for an electron of mass m_i; the regulated Green's function is then defined through

$$G_{Reg} = \sum_i a_i\, G(m_i) \quad , \tag{2.20}$$

where the coefficients a_i are chosen such that

$$\sum a_i = \sum a_i m_i^2 = 0$$

and

$$a_1 = 1 , \qquad m_1 = m_e \quad . \tag{2.21}$$

With G replaced by G_{Reg} in eq. (2.6), the limit $\underset{\sim}{x}' \to \underset{\sim}{x}$ exists, the integral over z converges, and there is no ambiguity associated with the interchange of those operations. Furthermore, the steps leading to the subsequent equations of section 2A, which include the changing of the original contour of integration C to the imaginary axis I and expanding ρ_{VP} in terms of ρ_k and $\rho^n_{|k|}$, are permissible with G_{Reg}. After renormalization of the nuclear charge, the limits $m_i \to \infty$, $i \geq 2$, are taken and the unambiguous, gauge invariant result for ρ_{VP} is thus obtained to all orders in $Z\alpha$ and for each partial wave contribution.

On the other hand, if we consider the Feynman graphs for ρ_{VP} in the field of finite radius nuclei, it will be clear that regularization is needed only for the contributions from the first few orders in $Z\alpha$. The graph corresponding to the term linear in $Z\alpha$ (Fig. 2a) is well known to be quadratically divergent. It is also well known that the electron loop integral for orders $(Z\alpha)^n$, $n \geq 5$, is finite. The third order graph is a borderline case and will be considered in detail later. Of course, in addition to the electron loop integral, the graphs in Fig. 2 also involve integrals for each external potential. For bounded potentials, such as those due to nuclei of finite extent, these integrals are finite and, hence, do not introduce new singularities. This is most easily seen by considering the integrations

in momentum space, where the rapid decrease of the nuclear charge form factor insures the convergence of the integrals. However, for the point nucleus (constant form factor) considered by Wichmann and Kroll (8), additional singularities appear due to the singularity of the potential at $\underset{\sim}{x} = 0$. Thus, while regularization will always be needed for first order, for orders $(Z\alpha)^n$, $n \geq 5$, regularization will not be needed as long as nuclei of finite extent are considered.

Considering the contribution from order $(Z\alpha)^3$, the electron loop integral in Fig. 2b is seen to diverge logarithmically. It is well known, however, that this divergence is eliminated if gauge invariance is imposed on the Feynman amplitude or, alternately, if the graph is regulated with one auxiliary mass (15). Therefore, an ambiguity is expected in the calculation of ρ^3 with eq. (2.6) if some regularization is not performed. To see how this ambiguity arises in eq. (2.6), consider the calculation of ρ^3 for the case of a constant external potential V. This calculation is carried out in Appendix I. The results show that if the limit $\underset{\sim}{x}' \to \underset{\sim}{x}$ is taken first and then the contour integral is performed in eq. (2.6), then a non-gauge invariant result, $\rho^3 = V^3/3\pi^2$, is obtained.* On the other hand, if the contour integral is performed first and then the limit $\underset{\sim}{x}' \to \underset{\sim}{x}$ is taken, then the gauge invariant result, $\rho^3 = 0$, is obtained. Thus, the ambiguity expected from the third order Feynman graph shows up in eq. (2.6) as an ambiguity associated with the interchange of a limit and integral. This ambiguity is of course eliminated if the regulator condition, eq. (2.21), with one auxiliary mass is applied to the

---

* See also Ref. (3) for a discussion of this point, and note that gauge invariance requires that $\rho^3 \to 0$ as $V \to$ constant.

Green's function. Note, by the way, that the calculation of the contribution from higher than third order is found in Appendix I to be free from this ambiguity, as it must be since the corresponding Feynman graphs are finite and unambiguous.

Although the calculation of ρ^3 in eq. (2.6) suffers from the above-mentioned ambiguity, the calculation of the contribution from each partial wave $\rho^3_{|k|}$ with eq. (2.19) is free from ambiguity. This is because the radial Green's function is much less singular than the full Green's function G. In particular, the limit $|\underset{\sim}{x}'| \to |\underset{\sim}{x}|$ exists for G_k while the limit $\underset{\sim}{x}' \to \underset{\sim}{x}$ does not exist for G. The results for the example of a constant external field considered in Appendix I confirm that $\rho^3_{|k|}$ is indeed free from ambiguity and thus automatically satisfies gauge invariance. Note, on the other hand, that the calculation of the first order density $\rho^1_{|k|}$ is ambiguous with eq. (2.19) since different results are obtained if the limit $r' \to r$ and the contour integral are interchanged. For third order, though, the calculation of ρ^3 by summing $\rho^3_{|k|}$ gives the unambiguous, gauge invariant result, $\rho^3 = 0$, for the case of a constant external potential.

This study of ρ^3 in a constant potential suggests that for bounded potentials, regularization of ρ^3 is achieved by calculating ρ^3 as a sum over the partial wave contributions $\rho^3_{|k|}$. In particular, each $\rho^3_{|k|}$ is expected to be well defined and gauge invariant. Therefore, the total charge contained in each partial wave density is expected to vanish.* Provided that the sum over k converges

---

* For undercritical potentials $(Z < Z_{cr})$.

fast enough, the sum of $\rho^3_{|k|}$ should then give the regularized result for ρ^3.

The convergence of the sum over k has been discussed in Ref. (1) based on the results of Wichmann and Kroll (8).* It was found that the lowest partial wave, $|k| = 1$, contains already 93% of the contribution to ρ^3 from all partial waves. Thus the sum over k is expected to converge very rapidly. In fact, for the VP density ρ^{5+}, for orders five and higher, the contribution from $|k| = 1$ amounts to more than 99% of the contribution from all k. Therefore, one expects that a good approximation for ρ^{3+} is obtained by calculating only the lowest partial wave contribution $\rho^{3+}_{|k|}$, $|k| = 1$, where

$$\rho^{3+}_{|k|}(r) = \frac{|e||k|}{2\pi}\left\{\sum_{k=\pm|k|}\ \sum_{-m_e<E<0} |\psi_{E,k}(r)|^2 + \frac{\mathrm{Re}}{\pi}\int_0^\infty dy\ \mathrm{Tr}\left[G_k(Z\alpha;\ r,r;\ iy) - G_k(-Z\alpha;\ r,r;\ iy) - 2\ Z\alpha\ G_k^{\,1}(r,r;\ iy)\right]\right\} . \tag{2.22}$$

This equation follows from removing the first order contribution, eq. (2.19), from $\rho_{|k|}$ in eq. (2.14). As it stands, eq. (2.22) is expected to require no further regularization for bounded potentials. Indeed, the explicit calculation of $\rho^{3+}_{|k|}$, $|k| = 1$, reported in Refs. (1,2) for finite radius nuclei confirms this expectation.

---

* See also Ref. (16).

For the first order (Uehling) contribution, the regulated VP density in an arbitrary potential is known (17,18). The energy shifts due to the Uehling potential have been worked out in detail for muonic atoms (3,19) and for superheavy electronic atoms (6,20) and, thus, need no further consideration here.

We now turn to the construction of $\mathrm{Tr}\, G_k$, $\mathrm{Tr}\, G_k^{\,1}$, and $\mathrm{Tr}\, G_k^{\,3}$, necessary for the calculation of the energy shifts quoted in Ref. (1,2) due to higher order VP.

3. Construction of $\mathrm{Tr}\, G_k$

The power of the Wichmann-Kroll formalism is that the radial Green's functions needed in eq. (2.22) can be readily constructed in terms of two particular solutions of the radial Dirac equation.* Let ψ_R be the solution regular at $r = 0$ and ψ_I be the solution regular at $r = \infty$ (i.e., $\psi_I \to 0$ as $r \to \infty$). Then for an eigenvalue k and energy z, these two component wavefunctions satisfy

$$\begin{bmatrix} 1 + V(r) - z & -\frac{1}{r}\frac{d}{dr} r + \frac{k}{r} \\ \frac{1}{r}\frac{d}{dr} r + \frac{k}{r} & -1 + V(r) - z \end{bmatrix} \begin{bmatrix} \psi_1(r) \\ \psi_2(r) \end{bmatrix} = 0 \,, \qquad (3.1)$$

where the radius and energy have been scaled by the electron mass. Then in terms of these solutions the radial Green's function is given by,

$$G_k(r,r';\, z) = \frac{1}{J(z)} \left\{ \theta(r' - r)\, \psi_R(r)\, \psi_I(r')^T + \theta(r - r')\psi_I(r)\psi_R(r')^T \right\}, \qquad (3.2)$$

---

* See also Ref. (21).

with the Wronskian $J(z)$ given by

$$J(z) = r^2 \left\{ \psi_{R2}(r)\, \psi_{I1}(r) - \psi_{R1}(r)\, \psi_{I2}(r) \right\} , \qquad (3.3)$$

and where T stands for transpose and the subscripts 1 and 2 refer to the upper and lower components. It is easy to verify from eq. (3.1) that $J(z)$ is independent of r and that G_k does satisfy eq. (2.9) for $m_e = 1$.

From eq. (3.2), we get

$$\mathrm{Tr}\, G_k(r,r';\, z) = \frac{\psi_I(r_>)^T\, \psi_R(r_<)}{J(z)} , \qquad (3.4)$$

where $r_>$ $(r_<)$ is the greater (lesser) of r and r'. The potential due to a nucleus of finite extent is of the form

$$V(r) = -Z\alpha \begin{cases} f(r/R)/R , & r < R \\ 1/r , & r > R \end{cases} . \qquad (3.5)$$

Two models of the nuclear charge distribution will be considered in this paper: Model I, a shell density, $\rho_{Nuc} = \delta(r - R)/4\pi R^2$, $f(r/R) = 1$; Model II, a uniform density, $\rho_{Nuc} = \theta(R - r)/(4\pi R^3/3)$, $f(r/R) = \left(3 - (r/R)^2\right)/2$.

The solutions of eq. (3.1) for the potential of eq. (3.5) are constructed by matching the interior solutions $(r < R)$ to the exterior solutions $(r > R)$ with a continuity condition at $r = R$.

The exterior solutions satisfy eq. (3.1) for the case of a pure Coulomb potential $(R = 0)$. These solutions are well known (8,12). Letting $\mathcal{N}$ denote the solution regular at $r = 0$ and $\mathcal{W}$ denote the solution regular at $r = \infty$, then

$$\begin{cases} \mathcal{M}_1 = \dfrac{1+z}{r^{3/2}} \left[(s-\nu)\, M_{\nu-\frac{1}{2},s}(2cr) - (k-\gamma/c)\, M_{\nu+\frac{1}{2},s}(2cr) \right] \\[2ex] \mathcal{M}_2 = \dfrac{c}{r^{3/2}} \left[(s-\nu)\, M_{\nu-\frac{1}{2},s}(2cr) + (k-\gamma/c)\, M_{\nu+\frac{1}{2},s}(2cr) \right] \end{cases}$$

and

$$\begin{cases} \mathcal{W}_1 = \dfrac{1+z}{r^{3/2}} \left[(k+\gamma/c)\, W_{\nu-\frac{1}{2},s}(2cr) + W_{\nu+\frac{1}{2},s}(2cr) \right] \\[2ex] \mathcal{W}_2 = \dfrac{c}{r^{3/2}} \left[(k+\gamma/c)\, W_{\nu-\frac{1}{2},s}(2cr) - W_{\nu+\frac{1}{2},s}(2cr) \right] \end{cases} , \qquad (3.6)$$

where

$$\gamma = Z\alpha , \qquad s = \sqrt{k^2 - \gamma^2} ,$$

$$c = \sqrt{1 - z^2} , \qquad \nu = \gamma \frac{z}{c} . \qquad (3.7)$$

The branch of the square root for c is taken such that $\mathrm{Re}[c] \geq 0$. The functions $M_{\alpha,\beta}$ and $W_{\alpha,\beta}$ in eq. (3.6) are the Whittaker (confluent hypergeometric) functions as defined in Ref. [22].

To obtain the interior solutions, the nuclear charge density must be specified. The simplest case for which the interior solutions are known is the shell distribution of model I. In that case, the interior potential is a constant $V_0 = -\gamma/R$. The solutions of eq. (3.1) for a constant potential V_0 are obtained from the solutions of eq. (3.1) with $V = 0$ simply by shifting the energy from z to $z - V_0$. Denoting the solution regular at $r = 0$ by u and the solution regular at $r = \infty$ by v for the case $V = 0$, we find [12]

$$\begin{cases} u_1 = (1 + z)\, j_{|k+\frac{1}{2}|-\frac{1}{2}}(icr) \\ u_2 = ic \dfrac{k}{|k|}\, j_{|k-\frac{1}{2}|-\frac{1}{2}}(icr) \end{cases}$$

and

$$\begin{cases} v_1 = -c\, h^{(1)}_{|k+\frac{1}{2}|-\frac{1}{2}}(icr) \\ v_2 = i(z - 1) \dfrac{k}{|k|}\, h^{(1)}_{|k-\frac{1}{2}|-\frac{1}{2}}(icr) \end{cases} , \qquad (3.8)$$

where j_ν and $h^{(1)}_\nu$ are the spherical Bessel and Hankel functions as defined in Ref. (23). The solutions of eq. (3.1) with $V = -\gamma/R$ are then given by

$$\tilde{u} = u(z + \gamma/R)$$

and

$$\tilde{v} = v(z + \gamma/R) \quad . \qquad (3.9)$$

Thus, the solutions of eq. (3.1) for a model I nucleus are given by

$$\psi_R = \theta(R - r)\tilde{u} + \theta(r - R)\left[a\mathcal{M} + b\mathcal{W}\right]$$

$$\psi_I = \theta(R - r)\left[\tilde{a}\tilde{u} + \tilde{b}\tilde{v}\right] + \theta(r - R)\mathcal{W} \quad . \qquad (3.10)$$

where the coefficients a, b, $\tilde{a}$, and $\tilde{b}$ are determined by the continuity condition at $r = R$. As in eq. (3.3), we define the bracket-expression for two arbitrary wavefunctions as

$$[\psi,\phi]_R \equiv R^2(\psi_2\phi_1 - \psi_1\phi_2)\Big|_{r=R} .$$

The coefficients in eq. (3.9) can then be expressed as

$$a = [\tilde{u},\mathcal{W}]_R/[\mathcal{M},\mathcal{W}]_R$$

$$b = [\mathcal{M},\tilde{u}]_R/[\mathcal{M},\mathcal{W}]_R$$

$$\tilde{a} = [\mathcal{W},\tilde{v}]_R/[\tilde{u},\tilde{v}]_R$$

$$\tilde{b} = [\tilde{u},\mathcal{W}]_R/[\tilde{u},\tilde{v}]_R \quad . \tag{3.11}$$

This form for the coefficients is partiuclarly useful because the different brackets are related to the Wronskians for different potentials. In particular, the Wronskian J_{coul} for a pure Coulomb potential is given by (see Appendix II)

$$J_{coul}(z) = [\mathcal{M},\mathcal{W}]_R = 4(1 + z)c^2 \frac{\Gamma(2s + 1)}{\Gamma(s - \nu)} \quad . \tag{3.12}$$

The Wronskian J_{V_0} for a constant potential is given by

$$J_{V_0}(z) = [\tilde{u},\tilde{v}]_R = 1 \quad , \tag{3.13}$$

as may be verified with eq. (10.1.31) of Ref. [23].

Finally, the Wronskian for the potential of eq. (3.5) as computed via inserting eq. (3.10) into eq. (3.3) is given by

$$J(z) = [\tilde{u},\mathcal{W}]_R = R^2(\tilde{u}_2\mathcal{W}_1 - \tilde{u}_1\mathcal{W}_2)\Big|_{r=R} \quad . \tag{3.14}$$

The zeroes of $J(z)$ determine the location of the poles of $\mathrm{Tr}\, G_k$ corresponding to bound states of the radial Hamiltonian with the potential of eq. (3.5). Note that the condition $J_{coul}(z) = 0$ gives the usual Sommerfeld's fine structure formula for a point nucleus.

The radial Green's function for several potentials of interest can now be constructed via eq. (3.2). The free radial Green's function $G_k^{\,0}$ referred to in eq. (2.15) is given by

$$G_k^{\,0}(r,r';\, z) = \theta(r' - r)\, u(r)\, v(r')^T + \theta(r - r')\, v(r)\, u(r')^T \quad , \tag{3.15}$$

in terms of the solutions in eq. (3.8). The pure Coulomb Green's function G_k^{coul} is given by (8,12)

$$G_k^{coul}(r,r';\, z) = \Big\{\theta(r' - r)\, \mathcal{M}(r)\, \mathcal{W}(r')^T + \theta(r - r')\, \mathcal{W}(r)\, \mathcal{M}(r')^T\Big\} / J_{coul}(z) \quad , \tag{3.16}$$

in terms of eqs. (3.6) and (3.12). Finally, for the case of a finite radius nucleus, G_k is given by substituting eq. (3.10) into eq. (3.2). The trace of G_k for $r' = r$, appearing in eq. (2.22), can be written conveniently for the case of a model I nucleus as

$$\mathrm{Tr}\, G_k(r,r\,;\, z) = \begin{cases} \mathrm{Tr}\, G_k^{\,0}(r,r;\ z + \gamma/R) + \mathrm{Tr}\, \Delta G_k^{\,<}, & r < R \\ \\ \mathrm{Tr}\, G_k^{coul}(r,r;\ z) + \mathrm{Tr}\, \Delta G_k^{\,>}\,, & r > R \quad , \end{cases} \tag{3.17}$$

where the finite size corrections $\Delta G_k^{<(>)}$ are given by

$$\mathrm{Tr}\ \Delta G_k^{<}(r,r;\ z) = \tilde{a}\ \tilde{u}(r)^T\ \tilde{u}(r)/J(z)$$

and

$$\mathrm{Tr}\ \Delta G_k^{>}(r,r;\ z) = b\,\mathcal{W}(r)^T\ \mathcal{W}(r)/J(z) \quad . \tag{3.18}$$

In this form, the expected properties of $\mathrm{Tr}\ G_k$ that

$$\mathrm{Tr}\ G_k \rightarrow \mathrm{Tr}\ G_k^0 \qquad \text{as} \qquad R \rightarrow \infty$$

and that for $\gamma < 1$, i.e., $Z < 137$,

$$\mathrm{Tr}\ G_k \rightarrow \mathrm{Tr}\ G_k^{coul} \qquad \text{as} \qquad R \rightarrow 0 \tag{3.19}$$

are easily derived from the asymptotic behavior of $\tilde{a}$ as $R \rightarrow \infty$ and of b as $R \rightarrow 0$ (see Appendix II). Note, however, that for $\gamma > 1$, the limit $R \rightarrow 0$ does not exist, confirming the result that for superheavy nuclei $(Z > 137)$, nuclear size effects must be taken into account (6).

Furthermore, the nuclear size correction to the VP density is computed directly from $\mathrm{Tr}\ \Delta G_k^{>}$ in eq. (3.18). This calculation is discussed in section 5.

The bound state wave functions appearing in eq. (2.22) are computed from the residues of $\mathrm{Tr}\ G_k$ for poles in the energy range $-m_e < E < 0$. As noted before, the location of these poles is determined by the condition $J(z) = 0$ for the Wronskian in eq. (3.14). The residues at those poles are seen from eqs. (3.17, 3.18) to come only from the finite size corrections, $\mathrm{Tr}\ \Delta G_k^{>(<)}$. These residues are

proportional to $|\tilde{u}(r)|^2$ for $r < R$ and to $|\mathcal{W}(r)|^2$ for $r > R$. This is expected since the bound state wavefunctions must be regular both at $r = 0$ and $r = \infty$. Furthermore, the continuity of the wavefunctions at $r = R$ is insured by the choice of $\tilde{a}$ and b and may easily be verified with eqs. (3.11, 3.14, 3.18). Note that the construction of G_k in eq. (3.2) also guarantees that these wavefunctions are normalized to unity. See section 6 for further discussion on the calculation of the $1S_{1/2}$ and $2P_{1/2}$ wavefunctions.

4. Construction of $\mathrm{Tr}\, G_k^{\,1}$ and $\mathrm{Tr}\, G_k^{\,3}$

In this section the trace of the radial Green's function to first and third order in $\gamma = Z\alpha$ are constructed from eq. (2.16). The $\mathrm{Tr}\, G_k^{\,1}$ is of course necessary for the calculation of $\rho^{3+}_{|k|}$ in eq. (2.22). The trace $\mathrm{Tr}\, G_k^{\,3}$, for $k = -1$, is calculated (1) to provide a check on the numerical calculation of $\rho_1^{\,3+}$ to third order, (2) to estimate the dependence of $\rho_1^{\,3+}$ on different models of the nuclear charge density, and (3) to determine the size of the contribution of $\rho_1^{\,3}$ to ρ^3. The ratio of the $|k| = 1$ contribution to the $|k| \geq 2$ contribution for the third order term is considered in order to estimate the accuracy of the approximation used in Refs. (1,2) for calculating the nuclear size effect by including only the $|k| = 1$ contribution to ρ^{3+}.

The construction of $\mathrm{Tr}\, G_k^{\,1}$ and $\mathrm{Tr}\, G_k^{\,3}$ will be carried out first generally for all k and then specifically for $|k| = 1$. To simplify the notation, define

$$(uu)_r = u(r)^T u(r)$$

$$(uv)_r = u(r)^T v(r) = v(r)^T u(r)$$

$$(vv)_r = v(r)^T v(r) \quad . \tag{4.1}$$

From eq. (2.16), $\mathrm{Tr}\, G_k^{\,1}$ is seen to involve the trace of a product of two free radial Green's functions $G_k^{\,0}$. This trace is easily calculated from eq. (3.15) to be

$$\mathrm{Tr}\Big(G_k^{\,0}(r,r_1)\, G_k^{\,0}(r_1,r)\Big) = (vv)_{r_>}\, (uu)_{r_<} \quad , \tag{4.2}$$

where $r_<$ $(r_>)$ is the lesser (greater) of r and r_1. Thus,

$$\mathrm{Tr}\, G_k^{\,1}(r,r;\, z) = (vv)_r \int_0^r dr_1\, r_1^{\,2}\, V(r_1)\, (uu)_{r_1}$$

$$+ (uu)_r \int_r^\infty dr_1\, r_1^{\,2}\, V(r_1)\, (vv)_{r_1} \quad . \tag{4.3}$$

To third order, $\mathrm{Tr}\, G_k^{\,3}$ involves the trace of a product of four free Green's functions. Let $T_4(r,r_1,r_2,r_3)$ denote this trace. The explicit analytic expression for T_4 depends on the relative ordering of the four radii. Consider, for example, the ordering in eq. (2.16) with $r > r_1 > r_2 > r_3$. From eq. (3.15),

$$T_4(r > r_1 > r_2 > r_3) = (vv)_r\, (uv)_{r_1}\, (uv)_{r_2}\, (uu)_{r_3} \quad . \tag{4.4}$$

Similar expressions may be written for the other 23 orderings. The contribution from the particular ordering in eq. (4.4) to $\mathrm{Tr}\, G_k^3$ will then be

$$(vv)_r \int_0^r dr_1\, r_1^2\, V(r_1) \int_0^{r_1} dr_2\, r_2^2\, V(r_2) \int_0^{r_2} dr_3\, r_3^2\, V(r_3)$$

$$\times\, (uv)_{r_1}\, (uv)_{r_2}\, (uu)_{r_3} \quad . \qquad (4.5)$$

The contributions from other orderings will have analogous forms. However, three other orderings, $(r > r_1 > r_3 > r_2)$, $(r > r_3 > r_1 > r_2)$, $(r > r_3 > r_2 > r_1)$, give rise to the same contribution as eq. (4.5). In fact, there are only eight different contributions to $\mathrm{Tr}\, G_k^3$ out of the possible 24.

From the following simple property,

$$\int_a^b dx\, f(x) \int_a^x dy\, f(y) = \frac{1}{2}\left\{\int_a^b dx\, f(x)\right\}^2 , \qquad (4.6)$$

all the occurring three dimensional integrals can be reduced to two dimensional ones and some two dimensional integrals reduce to one dimensional ones. Defining three fundamental integrals by

$$J_1(a,b) = \int_a^b dr\, r^2\, V(r)\, (uu)_r$$

$$J_2(a,b) = \int_a^b dr\, r^2\, V(r)\, (uv)_r$$

$$J_3(a,b) = \int_a^b dr\, r^2\, V(r)\, (vv)_r \quad , \qquad (4.7)$$

the eight different contributions to $\mathrm{Tr}\, G_k^{\,3}$ can be expressed in terms of the above integrals and the following six integrals

$$I_1 = \int_0^r dr_1\, r_1^{\,2}\, V(r_1)\, (uu)_{r_1}\, \tfrac{1}{2}\big(J_2(r_1,r)\big)^2$$

$$I_2 = \int_0^r dr_1\, r_1^{\,2}\, V(r_1)\, (vv)_{r_1}\, \tfrac{1}{2}\big(J_1(0,r_1)\big)^2$$

$$I_3 = \int_0^r dr_1\, r_1^{\,2}\, V(r_1)\, (uv)_{r_1}\, J_1(0,r_1)$$

$$I_4 = \int_r^\infty dr_1\, r_1^{\,2}\, V(r_1)\, (uv)_{r_1}\, J_3(r_1,\infty)$$

$$I_5 = \int_r^\infty dr_1\, r_1^{\,2}\, V(r_1)\, (vv)_{r_1}\, \tfrac{1}{2}\big(J_2(r,r_1)\big)^2$$

$$I_6 = \int_r^\infty dr_1\, r_1^{\,2}\, V(r_1)\, (uu)_{r_1}\, \tfrac{1}{2}\big(J_3(r_1,\infty)\big)^2 \quad . \tag{4.8}$$

Then $\mathrm{Tr}\, G_k^{\,3}$ is given by

$$\begin{aligned}\mathrm{Tr}\, G_k^{\,3}(r,r;\, z) \;=\; & (vv)_r \left\{4I_1 + 2I_2 + \left[J_1(0,r)\right]^2 J_3(r,\infty)\right\} \\ & + 4(uv)_r \left\{J_3(r,\infty)\, I_3 + J_1(0,r)\, I_4\right\} \\ & + (uu)_r \left\{4I_5 + 2I_6 + J_1(0,r)\left[J_3(r,\infty)\right]^2\right\} \quad . \end{aligned} \tag{4.9}$$

Note that in this notation eq. (4.3) can be written as

$$\mathrm{Tr}\, G_k^{\,1}(r,r;\, z) \;=\; (vv)_r\, J_1(0,r) + (uu)_r\, J_3(r,\infty) \quad . \qquad (4.10)$$

The reason that this notation is convenient is that analytic expressions may be obtained for the J_i, and thus, the calculation of $\mathrm{Tr}\, G_k^{\,3}$ involves only one dimensional numerical integrations. Also, $\mathrm{Tr}\, G_k^{\,1}$ can then be evaluated without any numerical integrations.

To proceed further, only the $k = -1$ radial Green's functions will be considered. Note that $\mathrm{Tr}\, G_k^{\,n}$ for $k = +1$ is related to the trace for $k = -1$ by eq. (2.18). From eq. (3.8), we get the following products for $k = -1$:

$$(uu)_r \;=\; (1 + z)^2 \frac{\sinh^2 cr}{(cr)^2} + \frac{1}{r^2}\left[\frac{\sinh cr}{cr} - \cosh cr\right]^2 \quad ,$$

$$(uv)_r \;=\; \frac{c\, e^{-cr}}{(cr)^2}\left\{(1 + z)\sinh cr + (1 - z)\left(1 + \frac{1}{cr}\right)\left[\frac{\sinh cr}{cr} - \cosh cr\right]\right\} \quad ,$$

$$(vv)_r \;=\; \frac{e^{-2cr}}{r^2}\left\{1 + \frac{(1 - z)^2}{c^2}\left(1 + \frac{1}{cr}\right)^2\right\} \quad . \qquad (4.11)$$

The fundamental integrals J_i may now be calculated for the two different models of the nuclear charge distribution considered in connection with eq. (3.5). Since the potential in eq. (3.5) has different forms for $r < R$ and $r > R$, it is natural to define the indefinite integrals $J_i^{<}$ and $J_i^{>}$ such that

$$\frac{d}{dr} J_1^{<}(r) = r^2 f(r/R) (uu)_r/R$$

$$\frac{d}{dr} J_2^{<}(r) = r^2 f(r/R) (uv)_r/R$$

$$\frac{d}{dr} J_3^{<}(r) = r^2 f(r/R) (vv)_r/R$$

and

$$\frac{d}{dr} J_1^{>}(r) = r (uu)_r$$

$$\frac{d}{dr} J_2^{>}(r) = r (uv)_r$$

$$\frac{d}{dr} J_3^{>}(r) = r (vv)_r \quad , \tag{4.12}$$

where $f(r/R) = 1$ for a model I nucleus and $f(r/R) = (3 - (r/R)^2)/2$ for a model II nucleus. Thus, for example,

$$J_2(a < R, b > R) = \left(J_2^{<}(R) - J_2^{<}(a)\right) + \left(J_2^{>}(b) - J_2^{>}(R)\right) \quad . \tag{4.13}$$

From eqs. (4.11, 41.2), the integrals for the case $k = -1$ and for a model I nucleus are easily verified to be

$$J_1^{<}(r) = \frac{1}{cR}\left\{\frac{1}{(1 - z)}\frac{1}{2}\sinh 2cr - \frac{z}{(1 - z)} cr - \frac{\sinh^2 cr}{cr}\right\}$$

$$J_2^{<}(r) = \frac{1}{cR}\left\{zr + \frac{e^{-2cr}}{2c} - \frac{1 - z}{c}\frac{e^{-cr}}{cr}\sinh cr - \frac{2z - 1}{2c}\right\} \quad ,$$

$$J_3^{<}(r) = \frac{-1}{cR}\frac{e^{-2cr}}{(1 + z)}\left\{1 + \frac{1 - z}{cr}\right\} \quad ,$$

Equation (4.14) continued next page

Equation (4.14) continued

$$J_1^{>}(r) = \frac{z}{(1-z)}\left\{\mathrm{Chi}(2cr) - \ln(2cr) - \gamma_E\right\}$$

$$+ \frac{1}{2}\left\{\frac{\sinh 2cr}{cr} - \frac{\sinh^2 cr}{(cr)^2} - 1\right\} \quad ,$$

$$J_2^{>}(r) = \frac{z}{c}\left\{E_1(2cr) + \ln(2cr) + \gamma_E\right\}$$

$$+ \frac{1-z}{c}\left\{\frac{e^{-2cr}}{2cr}\left(1 + \frac{1}{2cr}\right) - \frac{1}{(2cr)^2} + \frac{1}{2}\right\} \quad ,$$

$$J_3^{>}(r) = -\frac{2z}{(1+z)}E_1(2cr) - \frac{1-z}{1+z}\frac{e^{-2cr}}{cr}\left(1 + \frac{1}{2cr}\right) \quad , \qquad (4.14)$$

where γ_E is Euler's constant, E_1 is the exponential integral and Chi is the hyperbolic cosine integral defined in Ref. [23]. In this form the integrals $J_i^{<(>)}$ can be easily evaluated numerically (see section 7).

For model II nuclei, the interior integrals $J_k^{<}$ have a different form. These are related to $J_i^{<}$ in eq. (4.14) by

$$J_{III}^{<}(r) = \frac{1}{2}\left(3 - \left(\frac{r}{R}\right)^2\right)J_1^{<}(r) - \frac{1}{2(cR)^3}\left\{cr\left(\frac{2z\,(cr)^2}{3(1-z)} - 1\right)\right.$$

$$\left. + \frac{1}{8(1-z)}\left(e^{2cr}(1 - 2cr) - e^{-2cr}(1 + 2cr)\right) + \frac{1}{2}\sinh 2cr\right\}$$

Equation (4.15) continued next page

Equation (4.15) continued

$$J^{<}_{II2}(r) = \frac{1}{2}\left(3 - \left(\frac{r}{R}\right)^2\right) J_2^{<}(r) - \frac{1}{2(cR)^3}\left\{\frac{1-z}{c}\, cr\left(1 - \frac{2z\,(cr)^2}{3(1-z)}\right)\right.$$

$$\left. + \frac{e^{-2cr}}{2c}\left(cr - z + \frac{3}{2}\right) + \frac{1}{2c}\left(z - \frac{3}{2}\right) + (cr)^2\,\frac{2z-1}{2c}\right\} ,$$

$$J^{<}_{II3}(r) = \frac{1}{2}\left(3 - \left(\frac{r}{R}\right)^2\right) J_3^{<}(r) + \frac{1}{2(cR)^3}\,\frac{e^{-2cr}}{(1+z)}\left(cr - z + \frac{3}{2}\right) . \tag{4.15}$$

The integrals I_j may then be computed numerically for either nuclear model.

In order to estimate the ratio of the $|k| = 1$ contribution to the higher partial wave contribution for the third order VP density, the total VP charge accumulated at the origin for a point nucleus has to be calculated for $|k| = 1$. This charge is calculated through eq. (2) of Ref. (1). For that calculation, $\rho^3_{|k|}$ for $|k| = 1$ is needed in the limit $m_e \to 0$. To get the $m_e = 0$ limit for $\mathrm{Tr}\, G_k^{\,3}$, recall that in eqs. (4.11, 4.14, 4.15) the energy and radius have been scaled by the electron mass. In those equations the $m_e = 0$ limit is obtained by replacing $z \pm 1$ by z and c by $-iz$ in the upper half z plane and c by $+iz$ in the lower half z plane. With these substitutions, $\mathrm{Tr}\, G_k^{\,3}$ is computed as for the $m_e \neq 0$ case with eq. (4.9).

5. Finite Size Effects in Muonic Atoms

Having constructed all the relevant Green's functions for the calculation of the higher order VP density ρ^{3+}, we turn to a more detailed discussion of the effect of finite nuclear size on ρ^{3+}.

In particular, this section elaborates upon the calculations reported in Ref. (1) for muonic Pb.

For the region $r > R$, the correction to the trace of the Coulomb Green's function is given by $\mathrm{Tr}\,\Delta G_k^{>}$ in eq. (3.18). In this region, the difference, $\Delta\rho_k$, between the VP charge density for a finite radius nucleus and the density for a point nucleus is then given by eq. (2.11) with G_k replaced by $\Delta G_k^{>}$. In the discussion of section 2B, it was noted that the first order contribution has to be subtracted from G_k, as in eq. (2.22), to eliminate an ambiguity present in the calculation of the first order contribution to ρ_k. However, the calculation of the first order contribution to the difference $\Delta\rho_k$ for $r > R$ is free from ambiguity. To see this, consider the difference, $\mathrm{Tr}\,\Delta G_k^{1}(r,r')$, between $\mathrm{Tr}\,G_k^{1}(r,r')$ for a finite radius and point nucleus. From eqs. (2.16, 3.15, 4.12), we get for $r,r' > R$

$$\mathrm{Tr}\,\Delta G_k^{1}(r,r') = v(r)^T\, v(r')\left(J_1^{<}(R) - J_1^{>}(R)\right) , \qquad (5.1)$$

where it was noted that $J_1^{<}(0) = J_1^{>}(0) = 0$. It is easy to verify from eq. (3.8) that as a function of z, $\mathrm{Tr}\,\Delta G_k^{1}(r,r')$ decreases exponentially as $\exp\left(-|y|(r + r' - 2R)\right)$ for $z = iy$, $|y| \to \infty$. For $r,r' > R$, then, this exponential decrease insures the uniform convergence of the contour integral in eq. (2.19) for r' in the neighborhood of r and thus eliminates the ambiguity associated with the $r' \to r$ limit. For $r,r' < R$, though, the ambiguity in the calculation of $\Delta\rho_k^{1}$ is still present because $\mathrm{Tr}\,\Delta G_k^{1}$ decreases exponentially only as $\exp(-|y(r - r')|)$ for that region and the

contour integral does not converge uniformly for r' in the neighborhood of r. Thus regularization is required for the calculation of $\Delta\rho_k^{\,1}$ in the region $r < R$.

Because we are interested in transitions in muonic atoms between states of high angular momentum, the calculation of $\Delta\rho_k$ for $r < R$ may be avoided and we can restrict our attention to the calculation of $\Delta\rho_k$ for $r > R$, where no regularization is required. This is due to the observation by Arafune (4) and Brown et al. (5) that the mean radii of the muonic states involved in high angular momentum transitions are much larger than R. Thus, the energy shifts due to $\Delta\rho_k$ should be quite insensitive to the actual distribution of the VP density inside the nucleus, $r < R$. Since after regularization the total charge $\Delta Q^{<}$ contained in the region $r < R$ must cancel the charge, $\Delta Q^{>}$, in the region $r > R$, the approximation of setting $\Delta\rho_k(r) = -\Delta Q^{>}\,\delta(r)/r^2$ for $r < R$, will generate only small errors in the calculation of energy shifts for high angular momentum muonic states. Therefore, the energy shifts due to the nuclear size corrections to the VP density are calculated from the density $\Delta\rho_{|k|}$ given by*

$$\Delta\rho_{|k|} = \begin{cases} \dfrac{|e|\,|k|}{(2\pi)^2} \displaystyle\int_{-\infty}^{\infty} dy\ \mathrm{Tr}\Big(\Delta G_k^{>}(\gamma;\, iy) - \Delta G_k^{>}(-\gamma;\, iy)\Big), & r > R \\[2ex] -\left[\displaystyle\int_R^{\infty} dr\ r^2\ \Delta\rho_{|k|}\right] \dfrac{\delta(r)}{r^2}\ , & r < R\ , \end{cases} \qquad (5.2)$$

---

* Note that this procedure is applicable only for $\gamma < 1$, so that ρ_{VP} for a pure Coulomb field is still defined.

where $\Delta G_k^>$ is evaluated with either $k = |k|$ or $k = -|k|$. The contribution $\Delta\rho^1_{|k|}$, linear in γ, is calculated from eq. (5.2) by replacing $\mathrm{Tr}\,\Delta G_k^>$ with the first order correction $\mathrm{Tr}\,\Delta G_k^1(r,r)$ in eq. (5.1).

The primary purpose of calculating $\Delta\rho_{|k|}$ in Ref. (1) was to check the accuracy of the approximations in Refs. (4,5) of setting $m_e = 0$ and expanding $\Delta\rho_{|k|}$ in powers of the radius R. These approximations are implemented by setting $m_e = 0$ in eq.(3.18) and expanding b in powers of R. Note that the function $f(R,z,m_e)$ defined in Ref. (1) is related to b in eq. (3.18) by $f(R,z,m_e) = b/J(z)$.*

The $m_e = 0$ approximation requires the $m_e \to 0$ limit of eqs. (3.6, 3.8). The $\mathcal{M}$ and $\mathcal{W}$ functions for $m_e = 0$ are obtained from eq. (3.6) by making the following substitutions: $z \pm 1 \to z$, $c \to \mp iz$ (-1 for $\mathrm{Im}\, z > 0$; +1 for $\mathrm{Im}\, z < 0$), and $k \pm \gamma/c \to k$. The u and v functions for $m_e = 0$ are obtained from eq. (3.8) by making the first two of the above substitutions. With these new functions, $\mathrm{Tr}\,\Delta G_k^>$ $(m_e = 0)$ is calculated as in eq.(3.18).

The further approximation of retaining only the lowest power of R in an expansion of $f(R,z,m_e = 0)$ is obtained by calculating the small R limit of $b/J(z)$ in eq. (3.18). For the case of a model I nucleus with radius R, the leading term in an expansion of $f(R,z,m_e = 0)$ in powers of R is given by (see Appendix II)

---

* Note a misprint in Ref. (1), p. 1395, line 30: $f(R,z,m_e) = 0$ should read $f(R,z,m_e = 0)$.

$$f(R,iy,m_e = 0) \approx \left[\frac{iA - \gamma/(s-k)}{1 - iA\,\gamma/(s-k)}\right] R^{2s}\,(2y)^{2s-3}$$

$$\times \left(\frac{s - i\gamma}{s}\right)\left(\frac{\Gamma(s - i\gamma)}{\Gamma(2s)}\right)^2 , \qquad (5.3)$$

where $iA = -\tilde{u}_2/\tilde{u}_1$, evaluated in the limit $m_e \to 0$ and $R \to 0$ from eqs. (3.8 and 3.9). With this formula, the integrals in eq. (5.2) may be evaluated analytically (4,5).

The nuclear size corrections $\Delta\rho_{|k|}$ to the VP density for $|k| = 1$ are listed in Table I for Pb ($Z = 82$, model I, $R = 5.5$ fm) as a function of the radial coordinate r. The range of r covered in the first column is $R < r < 500R$. The next three columns list $\Delta\rho_1$ for the following cases: (1) $m_e \neq 0$ in eq. (5.2), (2) $m_e = 0$, and (3) both $m_e = 0$ and lowest power in R/r. The first order density $\Delta\rho_1^{\,1}$ is then listed in the last column. The energy level shifts due to these corrections have been discussed in Ref. (1). Here we want to discuss the differences in $\Delta\rho_1$ as calculated within the different approximations. For $r/\lambda\!\!\!^{-}_e \ll 1$, $\Delta\rho_1 \approx \Delta\rho_1(m_e = 0)$ to a high degree of accuracy. In fact, the assertion in Ref. (4) that corrections to $\Delta\rho_1(m_e = 0)$ appear to order $(m_e r)^2$ is supported by our numerical results. On the other hand, the approximation of retaining only the lowest power of R as in eq. (5.3) is not particularly accurate for $r \approx R$. In fact, $\Delta\rho_1\big(m_e = 0, O(R/r)\big)$ is

smaller than $\Delta\rho_1(m_e \neq 0)$ by roughly a factor of 2 in that region. For $0.1 \lesssim r/\lambda\!\!\!^{-}_e \lesssim 0.5$, all three approximations are seen to give the same value of $\Delta\rho_1$ to within 10%. For $r/\lambda\!\!\!^{-}_e > 1$, the relative accuracy of the $m_e = 0$ approximation decreases, although the relative accuracy of the $O(R/r)$ approximation increases, i.e., $\Delta\rho_1(m_e = 0) \approx \Delta\rho_1\big(m_e = 0, O(R/r)\big)$ but $\Delta\rho_1(m_e \neq 0) \neq \Delta\rho_1(m_e = 0)$.

The inadequacy of the $O(R/r)$ approximation in the region $r \approx R$ for computing the charge density does not affect the accuracy of the energy shifts computed from $\Delta\rho_1\big(m_e = 0, O(R/r)\big)$ in Ref. (1) very much, because, as noted before, the overlap of the muonic wave-functions with the region $r < R$ is very small for the high angular momentum states (e.g., $5g_{9/2}, 4f_{7/2}$). The inadequacy of the $m_e = 0$ approximation for computing $\Delta\rho_1$ in the region $r > \lambda\!\!\!^{-}_e$ does not affect the computed energy shifts very much because $\Delta\rho_1$ is very small in that region and only a small fraction of the charge contained in $\Delta\rho_1$ in the region $r > R$ is contained in the region $r > \lambda\!\!\!^{-}_e$; this can also be seen by comparing $\Delta Q_{1,2}$ in Table III of Ref. (1). The region that determines the accuracy of the computed energy shifts is thus the intermediate region, where all three approximations give the same $\Delta\rho_1$ to within 10%.

Note that a test on the numerical integrations required for the construction of Table I is given by a comparison of the values for $\Delta\rho_1\big(m_e = 0, O(R/r)\big)$ in Table I to the values determined from the analytic formula (eq. (3)) of Ref. (5). These values were found to agree to better than four places throughout the range $R \leq r \leq 500R$.

In connection with Tables I and II of Ref. (1),* the VP densities $\rho^{3}_{|k|}$ and $\rho^{3+}_{|k|}$ for $|k| = 1$ from eqs. (2.19, 2.22) are needed. These are listed in Table II here. As disucssed in Ref. (1), $\rho^{3}_{|k|}$ and $\rho^{3+}_{|k|}$ are expected to agree to within 10% for Pb. It is indeed reassuring that the values of $\rho^{3}_{|k|}$ and $\rho^{3+}_{|k|}$ are in such close agreement, then, considering that they were obtained with totally different computational techniques. A more demanding test of the numerical accuracy of each VP density in Table II is given by the degree of cancellation between the charges Q^- contained in the region where that density is negative $(r \lesssim 60 \text{ fm})$ and the charge Q^+ contained in the region where the density is positive $(r \gtrsim 60 \text{ fm})$. As reported in Ref. (1), these charges were found to cancel to better than five decimal places for both $\rho_1{}^{3}$ and $\rho_1{}^{3+}$. See section 7 for further discussion of the numerical techniques employed in calculating these densities.

6. Vacuum Polarization in Heavy Ion Collisions

In this section some of the results reported in Ref. (2) for the case of $Z\alpha > 1$ are elaborated upon. Consider a nucleus of type I with a radius $R = 10$ fm. The evaluation of $\rho^{3+}_{|k|}$ in eq. (2.22) requires, for large Z, the determination of bound state wavefunctions with energies E between $-m_e < E < 0$. The energy eigenvalues determined from eq. (3.14) for this type of nucleus are plotted in Fig. 3 as a function of Z for the $1S_{1/2}$ and $2P_{1/2}$ electronic states. The curves for $R = 0$ and 0.1 fm are also shown for

---

* Note that in the last line of Table I in Ref. (1), the second column should read $|k| \geq 1$ rather than $|k| = 1$.

comparison. Figure 3 is included here to exhibit the range of $Z\alpha$ for which the $1S_{1/2}$ and $2P_{1/2}$ state are present in eq. (2.22) for the particular model of the nucleus chosen here. Also the slopes of the curves in Fig. 3 provide a measure of the accuracy of the computed $1S_{1/2}$ and $2P_{1/2}$ wavefunctions (2). We note that the energy eigenvalues in Fig. 3 are in general agreement with the results of calculations using more realistic models of the nucleus (6,20), and that the values of Z_{cr} and of the slope dE/dZ at Z_{cr} compare favorably with those obtained in other calculations (2). It can be seen that the $1S_{1/2}$ state is present in eq. (2.22) for range $1.275 \geq Z\alpha \geq 1.086$, and that the $2P_{1/2}$ state is present for the range $1.383 \geq Z\alpha \geq 1.254$.

The critical value of the nuclear charge Z_{cr}, where $E_{1S_{1/2}} = -m_e$, has been determined in two different ways. First the zeroes of $J(z)$ in eq. (3.14) have been determined as a function of $Z\alpha$ for $z = -m_e + \varepsilon$ with $\varepsilon/m_e = 0.05, 0.01, 0.001, 0.0001$. Then $(Z\alpha)_{cr}$ is determined from the extrapolation to $\varepsilon = 0$. This method gave the value $(Z\alpha)_{cr} = 1.274587$. The second method of calculating $(Z\alpha)_{cr}$ is based on deriving the asymptotic form of $J(z)$ for $z \to -m_e$ $(c \to 0, \nu \to -\infty)$ and determining the zeroes of $J(z)$ in that limit (24). From the relation between the upper and lower components of the radial wavefunctions obtained from eq. (3.1), it is easy to see that the condition $J(z) = 0$ is equivalent to

$$\left.\frac{w_1'}{w_1}\right|_{r=R} = \left.\frac{\tilde{u}_1'}{\tilde{u}_1}\right|_{r=R} , \tag{6.1}$$

where only the upper components of the inner and outer wavefunctions enter, and the prime denotes the derivative. This equations is convenient because the asymptotic limit $(z \to -m_e)$ of the left-hand side is calculable from the relation (24)

$$\lim_{\alpha\to\infty} \Gamma(\alpha + 1)\, W_{-\alpha,\beta}\left(\frac{x}{\alpha}\right) = 2\sqrt{x}\; K_{2\beta}(2\sqrt{x}) \quad , \tag{6.2}$$

valid for $2\beta \neq$ integer and for real $x > 0$. Thus

$$\frac{w_1'}{w_1} \xrightarrow[z\to -m_e]{} \frac{r\,\frac{d}{dr}\left\{\frac{1}{r}\,K_{2\beta}\left(\sqrt{8\gamma r}\right)\right\}}{K_{2\beta}\left(\sqrt{8\gamma r}\right)} \quad , \tag{6.3}$$

where the modified Bessel function $K_{2\beta}$ and its derivative are calculable from the relations (22)

$$K_{2\beta}(2\sqrt{x}) = \left(\frac{\pi}{4\sqrt{x}}\right)^{\frac{1}{2}} W_{0,2\beta}(4\sqrt{x})$$

and

$$\frac{d}{dx}\, W_{0,2\beta}(x) = \frac{1}{2}\, W_{0,2\beta}(x) - \frac{1}{x}\, W_{1,2\beta}(x) \quad . \tag{6.4}$$

The solution of eq. (6.1) in the limit $z = -m_e$ with eqs. (6.3 and 6.4) gives the value $(Z\alpha)_{cr} = 1.274588$ in very good agreement with the value determined from extrapolation. In addition to providing a check on the calculation of $(Z\alpha)_{cr}$, this agreement shows that the nontrivial relations eqs. (6.2, 6.4) are satisfied by the computed Whittaker functions to a high degree of accuracy. The comparison of $(Z\alpha)_{cr}$ from the two methods therefore provides one important test on

the accuracy of the numerical techniques for computing the $W_{\alpha,\beta}$ functions (see section 7).

The calculation of the $1S_{1/2}$ bound state wavefunction in the range $1.275 \geq Z\alpha \geq 1.086$ is necessary not only for the calculation of ρ_1^{3+} in eq. (2.22) but also for the calculation of the $1S_{1/2}$ energy shift due to the VP potential.* Figure 4 has $4\pi r^2|\psi_{1S_{1/2}}|^2$ plotted for several values of $Z\alpha$ in that range for the case of the model I nucleus with $R = 10$ fm under consideration here. As noted in Ref. (2), one test of the accuracy of the computed wavefunctions (computed from the residues of the radial Green's function as discussed in Section 3) is given by the value of their norm. As reported there, all $1S_{1/2}$ and $2P_{1/2}$ wavefunctions so computed were found to be normalized to better than one part per 10^5. Another, more qualitative test of the accuracy of these wavefunctions is given by the comparison of the slope dE/dZ obtained from Fig. 3 to the approximation $dE/dZ \approx -\alpha m_e \langle 1/r \rangle$, where the expectation value $\langle 1/r \rangle$ is evaluated from the computed wavefunctions. Table III lists the values of the slope dE/dZ obtained in the two ways. The good agreement in Table III gives further assurance that the $1S_{1/2}$ and $2P_{1/2}$ wavefunctions were correctly calculated. Finally, we note that the $1S_{1/2}$ wavefunctions in Fig. 4 are in good qualitative agreement with those calculated using more realistic models of the nucleus (20).

For the study of the stability and localization of the helium-like density ρ_{He} as a function of Z in the neighborhood of Z_{cr},

---

* See Table 1 of Ref. (2).

we note that for $Z < Z_{cr}$

$$\rho_{He} = -2|e||\psi_{1S_{1/2}}(r)|^2 + \rho_{VP}$$

$$= -2|e||\psi_{1S_{1/2}}(r)|^2 + \rho_1^{3+} + \tilde{\rho} \quad , \qquad (6.5)$$

where ρ_{VP} has been divided into two parts: ρ_1^{3+}, which includes the contribution from higher orders for $|k| = 1$, and $\tilde{\rho}$, which includes the first order (Uehling) and the higher order, $|k| \geq 2$ densities. It is clear that $\tilde{\rho}$ is a continuous function of Z for around Z_{cr}.* Furthermore, the Uehling contribution is known (17), and the ratio of $\rho^{3+}_{|k|}$ for $|k| \geq 2$ to ρ_1^{3+} is small (2). Thus, for the study of the continuity of ρ_{He} around Z_{cr} we may neglect $\tilde{\rho}$ in eq. (6.5). The curves for ρ_{He} given in Fig. 2a of Ref. (2) for $Z < Z_{cr}$ are thus obtained by adding to $-2|e||\psi_{1S_{1/2}}(r)|^2$ in Fig. 4 the VP density ρ_1^{3+} as computed from eq. (2.22). These VP densities are plotted in Fig. 5 for several values of $Z\alpha$ approaching $(Z\alpha)_{cr} = 1.27459$. Note that these densities were also used in connection with Table I of Ref. (2). For $Z > Z_{cr}$, the $1S_{1/2}$ wavefunction in eq. (6.5) is no longer present and ρ_{He} is computed directly from eq. (2.22) by setting $\rho_{He} = \rho_1^{3+}$. The continuity of ρ_{He} as a function of Z around Z_{cr} may be seen from Table IV, where ρ_{He} for several values of the radial coordinate are listed as a function of Z. This table is intended to supplement Figs. 2a and 2b in Ref. (2). The continuity of ρ_{He} has been expected on the basis of

---

* The first discontinuity of $\tilde{\rho}$ occurs for $Z = Z_{cr}(2P_{3/2})$, where the $2P_{3/2}$ state reaches the lower continuum. This value of Z is much large than $Z_{cr}(1S_{1/2})$ though (6).

general arguments presented by Muller et al. (7). What we have presented here are precise calculations demonstrating this fact.

7. Numerical Techniques

This section describes the numerical techniques that were used to evaluate the Green's functions constructed in sections 3 and 4.

The calculation of $\mathrm{Tr}\, G_k$ in eq. (3.17) requires the calculation of the Whittaker functions $M_{\alpha,\beta}$ and $W_{\alpha,\beta}$ in eq. (3.6). The techniques employed to calculate these functions are those discussed extensively in Ref. (13). With those techniques an accuracy of better than 10 decimal places is achieved for the range of the arguments needed in the present study. Tests on the accuracy of the subroutines for calculating these functions include verification that those functions satisfy particular recursion relations* and that they also satisfy eq. (3.12) to more than 10 decimal places for a large range of the arguments. Another test is described in section 6.

For the calculation of $\mathrm{Tr}\, G_k^{\,1}$ and $\mathrm{Tr}\, G_k^{\,3}$, the integrals $J_i^{\,>}$ in eq. (4.14) require the evaluation of exponential integrals $E_1(x)$ and $\mathrm{Chi}(x)$. These functions are computed from the power series representations eq. (5.1.11) and eq. (5.2.18) of Ref. (23) for $x \leq 1$ and from the techniques described in Ref. (25) for $x > 1$. The subroutines for these functions were tested against tabulated values in Ref. (26). Again, better than 10 place accuracy was achieved.

The calculation of the integrals I_j in eq. (4.8) requires a numerical integration. All numerical integrations were done with a Gauss-Legendre quadrature method (27). This method is

---

* See p. 303 and 304 of Ref. (22).

particularly suited for the integration of functions that are well approximated by polynomials of relatively low degree on a given interval. This is because an n point quadrature formula is designed to give the correct value of the integral for a polynomial of degree $2n - 1$. The accuracy of the numerical integration with an n point formula for an arbitrary function is customarily estimated from the variation of the value of that integral as n is varied. This procedure was followed in the present work. Thus, if the value of an integral changes only in the eleventh decimal place as n is increased to $n + 10$ or $n + 20$, then the numerical integration is considered to be accurate to ten places with the n point formula.

For the integrals required in eq. (4.8), modification of the integrands is required in order to achieve ten place accuracy with low n. This is because many of the integrands contain terms such as inverse powers or logarithms that are not directly suited for integration by Gauss-Legendre quadrature. However, thse terms are easy to isolate in each integrand, and the integral over those terms may be done analytically. The remainder of the integrand will contain only terms such as r^m or $r^m \log r$ for $m \geq 1$, for which Gauss-Legendre quadrature converges fast. To illustrate this procedure, consider the integral

$$I_5^{>}(a,b) = \int_a^b dy\, y\, (vv)_y\, J_2^{>}(y) \quad , \tag{7.1}$$

which is needed in the evaluation of I_5 in eq. (4.8). As $y \to 0$, the integrand is of the form

$$\frac{(1 - z)^2}{c^4 y^3} \left[\frac{2}{3}(2z + 1) y - (1 + z) \frac{c y^2}{2}\right] + O(1) \quad , \qquad (7.2)$$

as is easily seen from eqs. (4.11, 4.14). While Gauss-Legendre quadrature is not suitable for the terms exhibited in eq. (7.2), their integral is trivial to do analytically. Thus, I_5 is computed for $b < 1/c$ by

$$I_5^{>}(a,b) = \int_a^b dy \left\{ y(vv)_y J_2^{>}(y) - \frac{2z + 1}{(1 + z)^2} \frac{2}{3y^2} + \frac{1 - z}{c} \frac{1}{2y} \right\}$$

$$+ \frac{2z + 1}{(1 + z)^2} \frac{2}{3} \left[\frac{1}{a} - \frac{1}{b}\right] - \frac{1 - z}{c} \frac{1}{2} \ln(b/a) \quad . \qquad (7.3)$$

With eq. (7.3), the number of quadrature points n found necessary to achieve ten place accuracy for $I_5^{>}$ in the range $0 < a < b < 1/c$ was $n = 20$. For large values of the argument $(cy > 1)$, the integrand in eq. (7.1) behaves as

$$\frac{2(1 - z)z}{c^3} \frac{e^{-2cy}}{y} \ln(2cy) \quad . \qquad (7.4)$$

However, because the exponential dominates this term, the presence of the logarithm and inverse power do not effect the convergence of the numerical integration very much. In fact, ten place accuracy is achieved for $I_5^{>}(a,\infty)$ when $a > 1/c$ with a 30 point quadrature formula applied to $I_5^{>}(a,a + 20/c)$. Therefore, $I_5^{>}(a,\infty)$ for any $a > 0$ may be computed to ten place accuracy with a maximum of 50 evaluations of the integrand. This numerical integration is then very rapidly performed. There are altogether 19 integrals of this type that

are required for the calculation of the I_j in eq. (4.8). All integrals are handled in the manner of the above example.

A critical test of the accuracy of the so computed $\mathrm{Tr}\, G_k$, $\mathrm{Tr}\, G_k^{\,1}$, and $\mathrm{Tr}\, G_k^{\,3}$ with the techniques described above is given by the comparison of the right- and left-hand sides of the equation

$$\mathrm{Tr}\Big(G_k(\gamma;\, r,r;\, z) - G_k(-\gamma;\, r,r;\, z)\Big)$$

$$= 2\gamma \mathrm{Tr}\, G_k^{\,1}(r,r;\, z) + 2\gamma^3\, \mathrm{Tr}\, G_k^{\,3}(r,r;\, z) + O(\gamma^5) \quad . \qquad (7.5)$$

For a model I nucleus with $R = 10$ fm, the right- and left-hand sides were computed for $\gamma = Z\alpha = 0.001$ and $r = aR$ with $\{a = 0.01, 0.1, 0.3, 0.7, 1.0, 1.05, 2.0, 5.0, 10.0, 20.0, 50.0, 100.0, 1000.0\}$ and $z = iy$ with $\{y = 0.0, 0.5, 1.0, 2.0, 4.0, 10.0, 20.0, 40.0, 100.0, 500.0, 1000.0\}$. Better than ten place agreement was found between the two sides for the range of variables considered.

The contour integral along the imaginary axis, which is required for the calcualtion of $\rho^3_{|k|}$ and $\rho^{3+}_{|k|}$ in eqs. (2.19, 2.22), is performed by dividing the interval $(0, i\infty)$ into two or three segments and applying a 30 point quadrature formula on each interval. The integrands fall off roughly as $1/z^5$ rather than exponentially, and consequently, the 30 point formulas were found to give five place accuracy. Of course, such accuracy is still quite adequate for the applications described in Sections 5 and 6. The charge densities $\rho^3_{|k|}$ and $\rho^{3+}_{|k|}$ were calculated for 60 values of the radial coordinate in each of the intervals $0 \leq r \leq 30\ R$ and $30R \leq r \leq 500\ R$. The 60 values in each interval were chosen to

coincide with Gauss-Legendre quadrature points so that integrations involving the charge densities (in the calculation of energy shifts due to VP) could be done immediately.

Finally, we note that all numerical calculations were done with the CDC 7600 at the Lawrence Berkeley Laboratory.

Acknowledgments

The author most gratefully acknowledges Dr. P. J. Mohr for many discussions on the theoretical and numerical aspects of this problem. Helpful discussions with Dr. E. H. Wichmann, Dr. W. Greiner, Dr. W. J. Swiatecki, Dr. R. N. Cahn, and Dr. L. Wilets are also gratefully acknowledged.

Appendix I

The calculation of the VP density for the case of a constant external potential V is discussed here in detail. The purpose of this calculation is to supplement section 2B by illustrating the properties of the Green's function G that makes regularization of eq. (2.6) necessary.

The Green's function G^V for a constant potential V is obtained from the free Green's function G^0 simply by shifting the energy z to $z - V$, where G^0 is given by

$$G^0(\underset{\sim}{x},\underset{\sim}{x}';\, z) = (-i\alpha\cdot\nabla + \beta + z)\,\frac{e^{-c\Delta}}{4\pi\Delta} \quad , \tag{I.1}$$

where $\Delta = |\underset{\sim}{x} - \underset{\sim}{x}'|$ and $c = (1 - z^2)^{\frac{1}{2}}$, $\mathrm{Re}(c) \geq 0$. Then

$$G^V(\underset{\sim}{x},\underset{\sim}{x}';\, z) = G^0(\underset{\sim}{x},\underset{\sim}{x}';\, z - V) \quad . \tag{I.2}$$

From eq. (I.1), it is clear that the limit $\Delta \to 0$ does not exist. However, consider the Taylor series expansion of $\mathrm{Tr}\, G^V$ in powers of V:

$$\pi\, \mathrm{Tr}\, G^V(\underset{\sim}{x},\underset{\sim}{x}';\, z) = \frac{z\, e^{-c\Delta}}{\Delta} - V\left(\frac{1}{\Delta} + \frac{z^2}{c}\right) e^{-c\Delta}$$
$$+ \frac{V^2}{2}\left(\frac{3z}{c} + \frac{z^3}{c^3}(1 + c\Delta)\right) e^{-c\Delta}$$
$$- \frac{V^3}{6}\left(\frac{3}{c^5} + \Delta\left(6\,\frac{z^2}{c^2} + 3\,\frac{z^4}{c^4}\right) + \Delta^2\,\frac{z^4}{c^3}\right) e^{-c\Delta} + \cdots . \qquad (I.3)$$

From this expansion, the singularity of $\mathrm{Tr}\, G^V$ as $\Delta \to 0$ is seen to be confined to the terms of order zero and one in V. Note also that the contour integral along the imaginary axis does not converge absolutely until third order for $\Delta = 0$.

Consider now the calculation of the third order density ρ^3 as in eq. (2.8). Then in units of $-|e|$, ρ^3 is given by

$$\rho^3(\underset{\sim}{x}) = \frac{V^3}{12\pi} \int_{-\infty}^{\infty} dy\, \frac{d^3}{d(iy)^3} \left\{\mathrm{Tr}\, G^0(\underset{\sim}{x},\underset{\sim}{x}';\, iy)\right\}\Bigg|_{\underset{\sim}{x}'\to\underset{\sim}{x}}$$
$$= \frac{V^3}{6\pi^2}(-i) \lim_{z\to i\infty} \lim_{\Delta\to 0} \left\{\left(3\,\frac{z}{c} + \frac{z^3}{c^3}(1 + c\Delta)\right) e^{-c\Delta}\right\} . \qquad (I.4)$$

From eq. (I.4), it is clear that depending on which order the limits are taken, $\rho^3 = V^3/3\pi^2$ or 0. For higher orders, though, a similar calculation shows that $\rho^n = 0$ for $n \geq 4$ independently of the order of the limits.

To calculate the contribution $\rho_{|k|}$ to ρ_{VP} consider eq. (2.14). The trace $\mathrm{Tr}\, G_k^{\,V}$ is obtained from $\mathrm{Tr}\, G_k^{\,0}$ in eq. (3.15) again by shifting z to $z - V$. With reference to eqs. (3.4, 3.8, 3.13), we define

$$D^0_{|k|} \equiv \mathrm{Tr}\Big(G_k^{\,0}(r,r';\, z) + G_{-k}^{\,0}(r,r';\, z)\Big)$$

$$= -2zc\Big(j_+(icr_<)\, h_+^{(1)}(icr_>) + j_-(icr_<)\, h_-^{(1)}(icr_>)\Big) \quad , \text{(I.5)}$$

where $\pm$ stand for $|k \pm \frac{1}{2}| - \frac{1}{2}$. Then $D^V_{|k|} = D^0_{|k|}(z - V)$. Again a power series in V may be obtained by taking successive derivatives of $D^0_{|k|}$ with respect to z. Note that the $\Delta \to 0$ singularity is absent for each $|k|$ to any order in V. However, the calculation of the first order density $\rho^1_{|k|}$ in eq. (2.17) gives

$$\rho^1_{|k|}(r) = \frac{|k|V}{(2\pi)^2} \int_{-\infty}^{\infty} dy\, \frac{d}{d(iy)} \left[D^0_{|k|}(r,r';\, iy)\right]\Bigg|_{r'\to r}$$

$$= \frac{|k|V}{(2\pi)^2}(-2i) \lim_{z\to i\infty} \lim_{r'\to r} D^0_{|k|}(r,r';\, z) \quad . \qquad \text{(I.6)}$$

If the limit $r' \to r$ is taken first, then from the high z limit of eq.(I.5) for $r_< = r_>$, we get $\rho^1_{|k|} = |k|V/(\pi r)^2$. On the other hand, if $r' \neq r$, then since the product $j_\nu(icr_<)$ and $h_\nu^{(1)}(icr_>)$ decreases exponentially for $z \to i\infty$, we get $\rho^1_{|k|} = 0$. Thus there is an ambiguity associated with the calculation of $\rho^1_{|k|}$, and hence, regularization is required for first order. For higher orders, though, it is easy to verify that terms of even orders vanish because even derivatives of $D^0_{|k|}$ are odd functions of z and that terms of odd

orders vanish because the even derivatives vanish at $z = \pm i\infty$. Also there is no ambiguity associated with the interchange of limits for the terms of higher orders.

Appendix II

The properties of $\mathrm{Tr}\, G_k$ given in eq. (3.19) as well as the asymptotic form of $b/J(z)$ in eq. (5.3) are derived here.

First, from eqs. (3.11, 3.13), $\tilde{a} = [\mathcal{W}, \tilde{v}]_R$. Since both $W_{\alpha,\beta}(z)$ and $h_\nu^{(1)}(iz)$ in eqs. (3.6, 3.9) decrease exponentially for $\mathrm{Re}\,(z) \to \infty$ (23), it follows at once that $\tilde{a} \to 0$ as $R \to \infty$.

The calculation of b in eq. (3.11) in the small R limit is obtained from relations (22,23)

$$M_{\alpha,\beta}(x) = x^{\beta+\frac{1}{2}}\left(1 + O(x)\right)$$

$$W_{\alpha,\beta}(x) = \frac{\Gamma(2\beta)}{\Gamma(\beta + \frac{1}{2} - \alpha)}\, x^{-\beta+\frac{1}{2}}\left(1 + O(x)\right)$$

$$+ \frac{\Gamma(-2\beta)}{\Gamma(-\beta + \frac{1}{2} - \alpha)}\, x^{\beta+\frac{1}{2}}\left(1 + O(x)\right), \qquad \text{(II.1)}$$

for $x \to 0^+$. Note that eq. (3.12) follows from the calculation of $[\mathcal{M}, \mathcal{W}]_R$ with these relations. Restricting now to the case $\gamma < |k|$ (s is real), the ratio $b/J(z)$ in the small R limit may be written from eqs. (3.11, 3.12, 3.14, and II.1) as

$$b/J(z) = -\frac{(\tilde{u}_1 \mathcal{M}_2 - \tilde{u}_2 \mathcal{M}_1)}{(\tilde{u}_1 \mathcal{W}_2 - \tilde{u}_2 \mathcal{W}_1)} \frac{1}{J_{coul}(z)}$$

$$\underset{R\to 0}{\approx} \left\{ \frac{(s - \nu - k + \gamma/c)A - (s - \nu + k - \gamma/c)}{(-s + \nu + k + \gamma/c) - (s - \nu + k + \gamma/c)A} \right\}$$

$$\times \ (2cR)^{2s} \frac{\Gamma(s - \nu + 1)}{\Gamma(2s)} \frac{1}{J_{coul}(z)} \quad , \qquad \text{(II.2)}$$

where $A = (\tilde{u}_2/\tilde{u}_1)(1 + z)/c$. Note that corrections to the small R form in eq. (II.2) appear in orders R^{4s} and R^{2s+1}. For a model I nucleus, the small R limit of A is found from eqs. (3.8, 3.9) to be

$$A \underset{R\to 0}{\approx} \frac{1 + z}{c} \frac{k}{|k|} \frac{j_-(\gamma)}{j_+(\gamma)} \quad , \qquad \text{(II.3)}$$

where $j_\pm$ stand for $j_{|k\pm\frac{1}{2}|-\frac{1}{2}}$.

From eq. (II.2), the second property of $\mathrm{Tr}\, G_k$ in eq. (3.19) follows, since $\mathrm{Tr}\, \Delta G_k^{>} \to O(R^{2s}) \to 0$ as $R \to 0$. Note, however, that for $\gamma > 1$, $(Z > 137)$, s is purely imaginary for $|k| = 1$, and, thus, the limit $R \to 0$ does not exist.

Finally, eq. (5.3) is obtained by taking the $m_e \to 0$ limit in eq. (II.2). As described in section 5, this limit is taken by making the following substitutions: for $z = iy$, $y \geq 0$, $z \pm 1 \to iy$, $c \to y$, $\nu \to i\gamma$, $k \pm \gamma/c \to k$.

REFERENCES

(1) M. Gyulassy, Phys. Rev. Letters 32 (1974) 1393.

(2) M. Gyulassy, Vacuum Polarization in Heavy Ion Collisions, Lawrence Berkeley Laboratory preprint LBL-3079 (1974), to be published.

(3) G. A. Rinker, Jr. and L. Wilets, Phys. Rev. Letters 31 (1973) 1559.

(4) J. Arafune, Phys. Rev. Letters 32 (1974) 560.

(5) L. S. Brown, R. N. Cahn, and L. D. McLerran, Phys. Rev. Letters 32 (1974) 562.

(6) W. Pieper and W. Greiner, Z. Phys. 218 (1969) 327.

(7) B. Muller, J. Rafelski, and W. Greiner, Z. Phys. 257 (1972) 62; Z. Phys. 257 (1972) 183; Nuovo Cimento 18 (1973) 551; J. Rafelski, B. Muller, and W. Greiner, Nucl. Phys. B68 (1974) 585; L. Fulcher and A. Klein, Phys. Rev. D8 (1973) 2455; Ya. B. Zel'Dovich and V. S. Popov, Sov. Phys.-Usp. 14 (1972) 673.

(8) E. H. Wichmann and N. M. Kroll, Phys. Rev. 101 (1956) 843.

(9) J. D. Bjorken and S. D. Drell, Relativistic Quantum Fields (McGraw-Hill, New York, 1965).

(10) J. Schwinger, Phys. Rev. 82 (1951) 664.

(11) S. S. Schweber, An Introduction to Relativistic Quantum Field Theory (Row, Peterson and Company, Illinois, 1961).

(12) P. J. Mohr, Self-Energy Radiative Corrections in Hydrogen-Like Systems, Lawrence Berkeley Laboratory preprint LBL-2153 (1973), to appear in Annals of Phys.

(13) P. J. Mohr, Numerical Evaluation of the $1S_{\frac{1}{2}}$ State Radiative Level Shift, Lawrence Berkeley Laboratory preprint LBL-2154 (1973), to appear in Annals of Phys.

(14) W. Pauli and F. Villars, Rev. of Mod. Phys. 21 (1949) 434.

(15) R. Karplus and M. Neuman, Phys. Rev. 80 (1950) 380.

(16) L. S. Brown, R. N. Cahn, and L. D. McLerran, Vacuum Polarization in a Strong Coulomb Field I: Induced Point Charge, University of Washington preprint (1974).

(17) E. A. Uehling, Phys. Rev. 48 (1935) 55.

(18) J. Blomqvist, Nucl. Phys. B48 (1972) 95.

(19) R. Glauber, W. Rarita, and P. Schwed, Phys. Rev. 120 (1960) 609.

(20) G. Soff, B. Muller, and J. Rafelski, Precise Values for Critical Fields in Quantum Electrodynamics, University of Pennsylvania preprint (1974).

(21) B. Friedman, Principles and Techniques of Applied Math (John Wiley and Sons, Inc., New York, 1956).

(22) W. Magnus, F. Oberhettinger and R. P. Soni, Formulas and Theorems for the Special Functions of Mathematical Physics, Third ed. (Springer-Verlag, New York, 1966).

(23) Handbook of Mathematical Functions, ed. M. Abramowitz and I. A. Stegun, NBS Applied Mathematics Series (Washington, 1966).

(24) V. S. Popov, JETP 32 (1971) 526.

(25) W. J. Cody and H. C. Thacher, Jr., Math. Comp. 22 (1968) 641; Math. Comp. 23 (1969) 289.

(26) J. Miller and R. P. Hurst, Math. Comp. 12 (1958) 187.

(27) A. H. Stroud and D. Secrest, Gaussian Quadrature Formulas (Prentice-Hall, Englewood Cliffs, 1966).

Table I. The finite size correction to the $|k| = 1$ vacuum polarization density for Pb, $R = 5.5$ fm $= 1.42 \times 10^{-2}\,\lambda\!\!\!^{-}_e$. $\Delta\rho$ is given for three approximations: (1) $m_e \neq 0$, (2) $m_e = 0$ and (3) $m_e = 0, O(R/r)$. The first order correction $\Delta\rho^1$ is also listed for $m_e \neq 0$. The radius is measured in $\lambda\!\!\!^{-}_e$ and the quantities $r^2\Delta\rho$ are given in units of $-4\pi|e|/\lambda\!\!\!^{-}_e$.

r	$r^2\Delta\rho$	$r^2\Delta\rho(m_e=0)$	$r^2\Delta\rho\left(m_e=0,O(R/r)\right)$	$r^2\Delta\rho^1$
1.51×10^{-2}	8.15×10^{0}	8.15×10^{0}	4.35×10^{0}	8.05×10^{0}
4.56×10^{-2}	3.16×10^{-1}	3.16×10^{-1}	2.45×10^{-1}	2.74×10^{-1}
1.14×10^{-1}	2.56×10^{-2}	2.55×10^{-2}	2.28×10^{-2}	1.76×10^{-2}
2.99×10^{-1}	1.92×10^{-3}	1.92×10^{-3}	1.83×10^{-3}	9.55×10^{-4}
4.27×10^{-1}	7.39×10^{-4}	7.51×10^{-4}	7.26×10^{-4}	3.23×10^{-4}
6.95×10^{-1}	1.91×10^{-4}	2.09×10^{-4}	2.05×10^{-4}	6.99×10^{-5}
1.03×10^{0}	5.71×10^{-5}	7.43×10^{-5}	7.33×10^{-5}	1.82×10^{-5}
2.50×10^{0}	1.34×10^{-6}	7.33×10^{-6}	7.29×10^{-6}	3.15×10^{-7}
4.55×10^{0}	1.63×10^{-8}	1.55×10^{-6}	1.54×10^{-6}	3.13×10^{-9}
7.02×10^{0}	9.80×10^{-11}	4.99×10^{-7}	4.98×10^{-7}	1.64×10^{-11}

Table II. The $|k| = 1$ vacuum polarization density times r^2 for Pb (model I, $R = 5.5$ fm) in the range $0 < r < 500$ R. The contributions from third order and orders $n \geq 3$ are listed separately in units of $4\pi|e|/\lambda\!\!\!^{-}_e$ as functions of r (in units of $\lambda\!\!\!^{-}_e$).

r	$r^2\rho_1{}^3$	$r^2\rho_1{}^{3+}$
1.6875×10^{-4}	-1.8351×10^{-5}	-1.9439×10^{-5}
2.1817×10^{-3}	-3.0541×10^{-3}	-3.2450×10^{-3}
6.4730×10^{-3}	-2.5196×10^{-2}	-2.6746×10^{-2}
1.2997×10^{-2}	-7.7206×10^{-2}	-8.1857×10^{-2}
1.7075×10^{-2}	-9.2082×10^{-2}	-9.7962×10^{-2}
2.6808×10^{-2}	-7.4151×10^{-2}	-8.0434×10^{-2}
3.8554×10^{-2}	-4.6475×10^{-2}	-5.1769×10^{-2}
6.7561×10^{-2}	-1.5718×10^{-2}	-1.8589×10^{-2}
1.0285×10^{-1}	-4.4931×10^{-3}	-5.7939×10^{-3}
1.4290×10^{-1}	-7.5815×10^{-5}	-5.2797×10^{-4}
1.6417×10^{-1}	1.0772×10^{-3}	8.8277×10^{-4}
2.0810×10^{-1}	2.3900×10^{-3}	2.5152×10^{-3}
2.8439×10^{-1}	3.2348×10^{-3}	3.5907×10^{-3}
3.6762×10^{-1}	3.4147×10^{-3}	3.8399×10^{-3}
4.2081×10^{-1}	3.3712×10^{-3}	3.8013×10^{-3}
6.9479×10^{-1}	2.6325×10^{-3}	2.9663×10^{-3}
1.0313×10^{0}	1.7118×10^{-3}	1.9183×10^{-3}
2.0386×10^{0}	3.8784×10^{-4}	4.2928×10^{-4}
4.0348×10^{0}	1.6036×10^{-5}	1.7329×10^{-5}
5.5101×10^{0}	1.6088×10^{-6}	1.6946×10^{-6}
7.0200×10^{0}	1.9882×10^{-7}	2.0379×10^{-7}

Table III. Slope dE/dz of curves in Fig. 3 for $1S_{1/2}$ and $2P_{1/2}$ states for $R = 10$ fm compared to approximation $-\alpha m_e \langle 1/r \rangle$ in units of keV.

$Z\alpha$	$-dE/dz$	$\alpha m_e \langle 1/r \rangle$	state
0.95	8	8	$1S_{1/2}$
1.12	15	16	
1.205	21	22	
1.27445	27	28	
1.27445	25	26	$2P_{1/2}$
1.28	25	26	
1.295	27	28	
1.38	35	37	

Table IV. Computed values of $4\pi r^2 \rho_{He}(r)$ in units of $-|e|/\lambda\!\!\!^{-}_e$ as a function of $Z\alpha$ for different values of r (in units of $\lambda\!\!\!^{-}_e$). These values show the continuity of ρ_{He} around $(Z\alpha)_{cr} = 1.27459$.

$r \backslash Z\alpha$	1.2732	1.27445	1.27545	1.28
0.0036	0.1082	0.1091	0.1097	0.1124
0.0261	3.8384	3.8671	3.8901	3.9959
0.0681	6.4124	6.4495	6.4791	6.6144
0.1505	5.0467	5.0600	5.0705	5.1160
0.4035	1.6789	1.6726	1.6676	1.6448
1.0330	0.1852	0.1831	0.1815	0.1742

FIGURE CAPTIONS

Fig. 1. Singularities of the Green's function in the complex energy plane and contours C_0, C_{He}, and I giving the VP and helium-like charge densities in units of $|e|$.

Fig. 2. Feynman graphs corresponding to ρ_{VP} to lowest order (a) and higher orders (b) in $Z\alpha$, where X denotes the nuclear charge form factor.

Fig. 3. Energy eigenvalues for the $1S_{1/2}$ and $2P_{1/2}$ states as a function of $Z\alpha$ for a model I nucleus with $R = 0.0$, 0.1, and 10.0 fm.

Fig. 4. The $1S_{1/2}$ wavefunctions for several values of $\gamma = Z\alpha$ approaching $(Z\alpha)_{cr} = 1.27459$ for a model I, 10 fm nucleus.

Fig. 5. The $|k| = 1$ VP density for orders $(Z\alpha)^n$, $n \geq 3$, for several values of $\gamma = Z\alpha$ corresponding to Fig. 4.

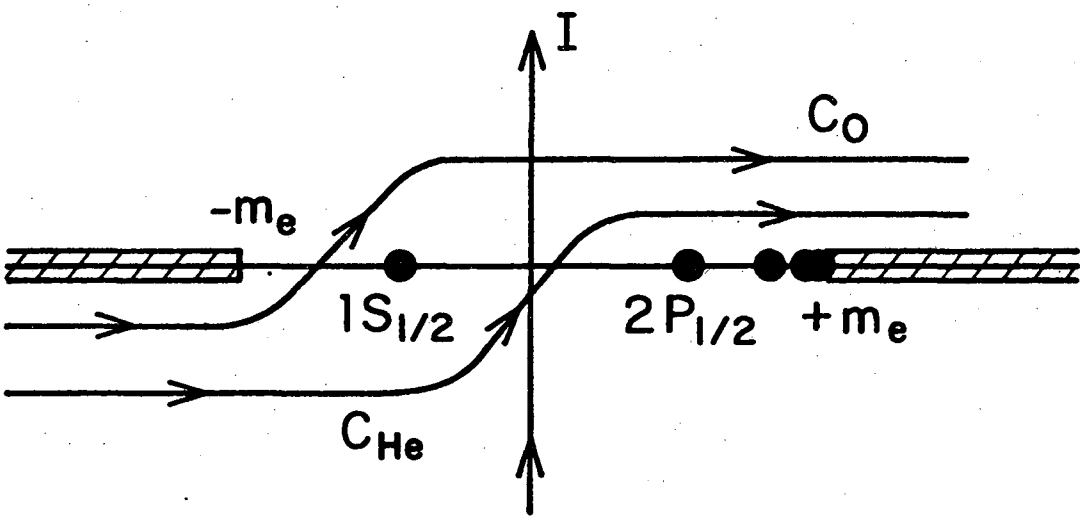

XBL 747-3588

Fig. 1

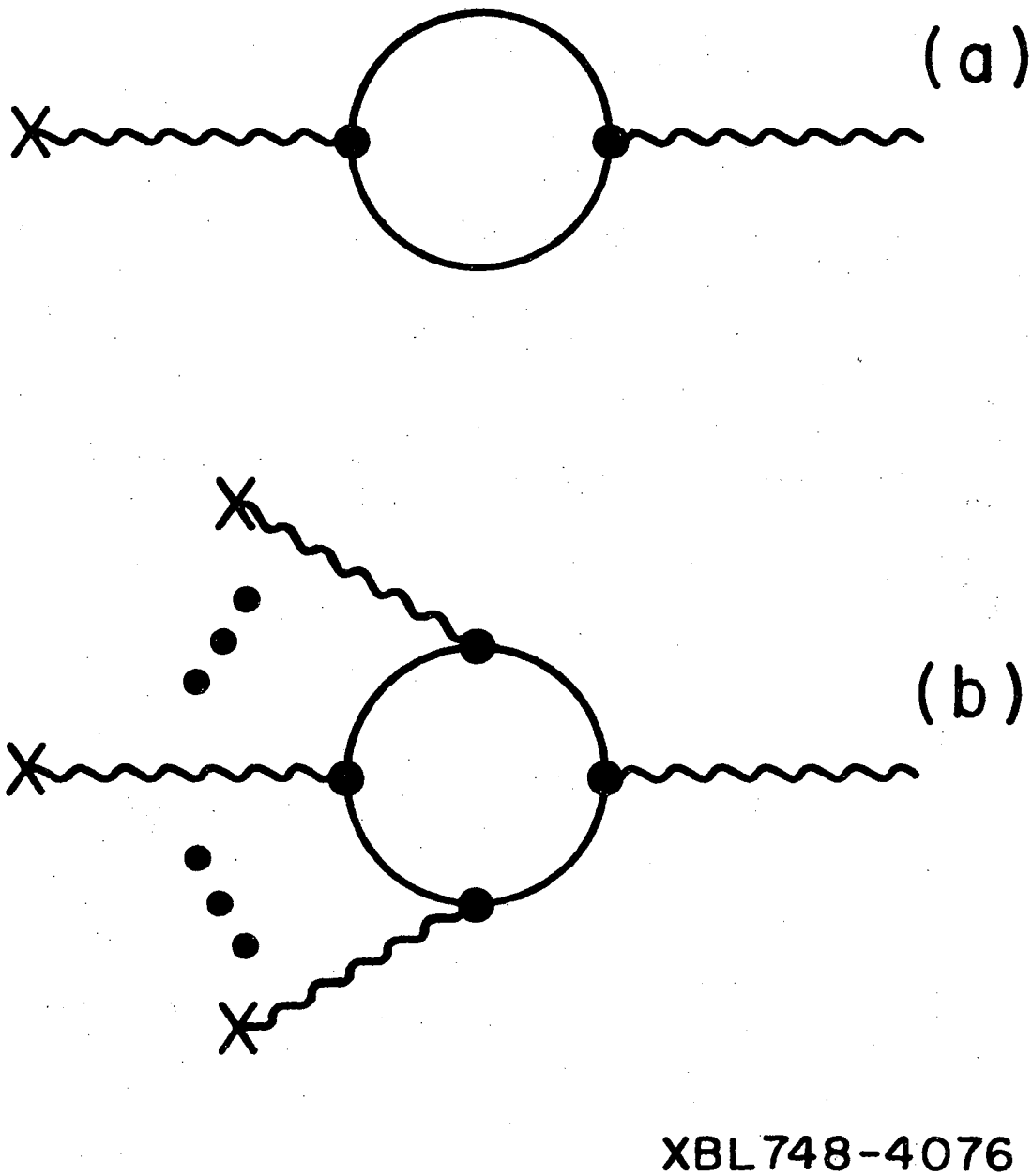

XBL748-4076

Fig. 2

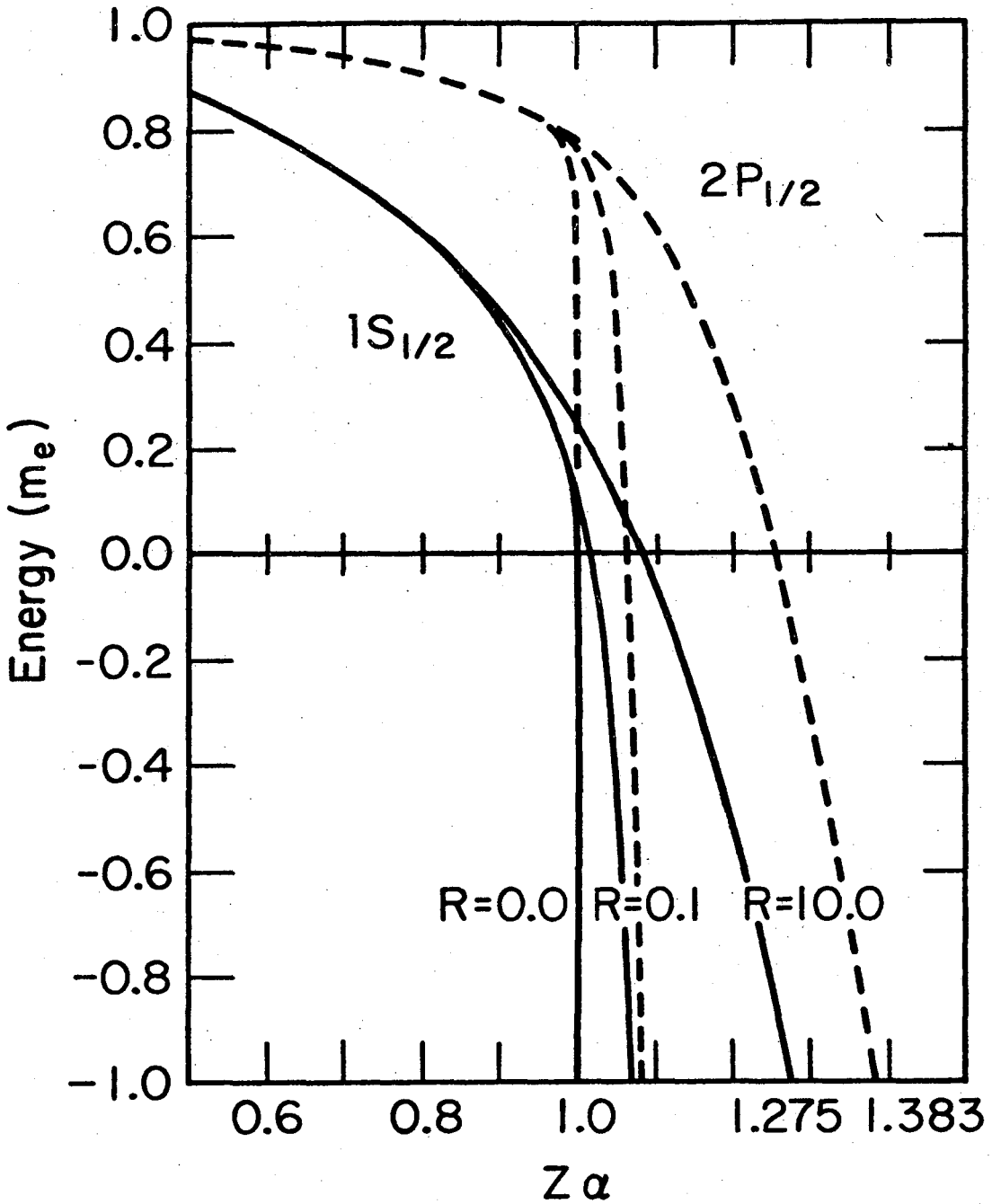

XBL 748-4073

Fig. 3

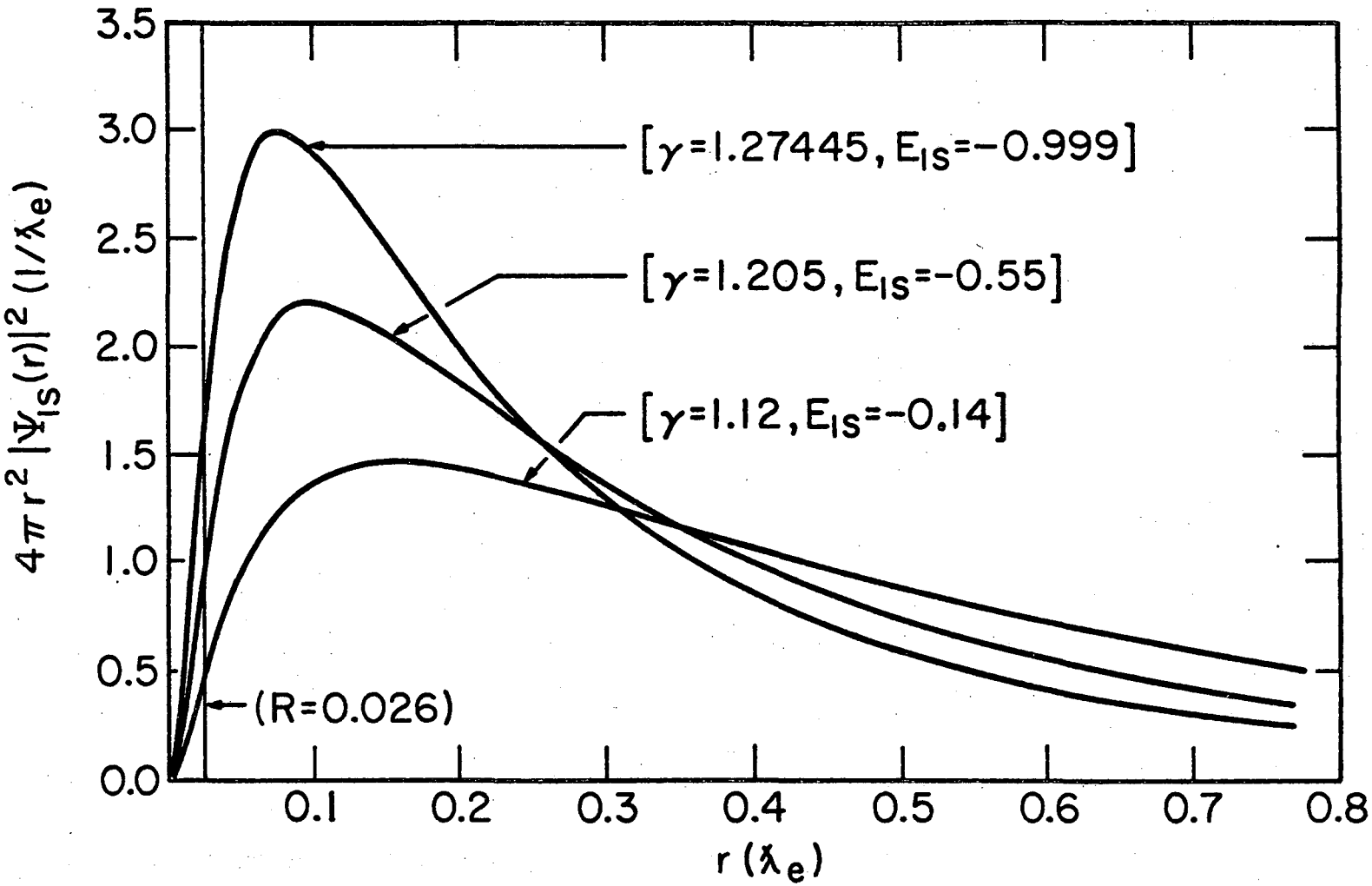

XBL 748-4074

Fig. 4

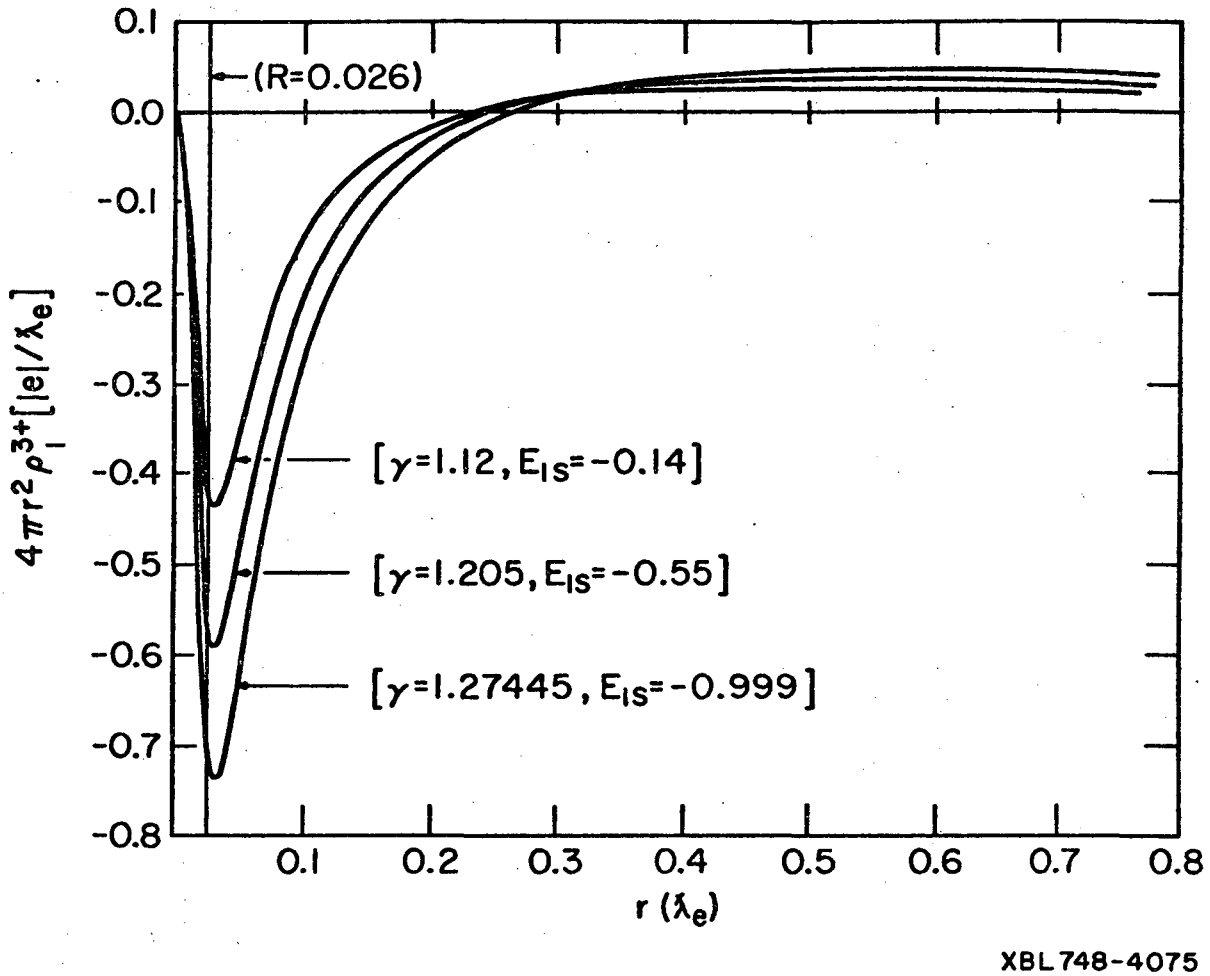
0.1
0.0
-0.1
-0.2
-0.3
-0.4
-0.5
-0.6
-0.7
-0.8
(R=0.026)
[γ=1.12, E1s=-0.14]
[γ=1.205, E1s=-0.55]
[γ=1.27445, E1s=-0.999]
4πr²ρ1³⁺[|e|/λe]
0.1
0.2
0.3
0.4
0.5
0.6
0.7
0.8
r (λe)
XBL748-4075

Fig. 5

0 0 0 0 4 2 0 4 2 1 6

ACKNOWLEDGMENTS

In addition to the acknowledgments at the end of each chapter, I would like to express my appreciation for the constant support and encouragement of my mother and of my wife throughout this research. I would especially like to thank my wife for her help in editing this manuscript.

I owe special thanks to Professor Mahiko Suzuki and Professor Stanley Mandelstam for their inspiring teaching and advice during my stay at Berkeley.

I am also grateful to Mrs. Christina Graham and Ms. Georgella Perry for their efforts in typing this manuscript.

0 0 0 0 4 2 0 4 2 1 7

LEGAL NOTICE

This report was prepared as an account of work sponsored by the United States Government. Neither the United States nor the United States Atomic Energy Commission, nor any of their employees, nor any of their contractors, subcontractors, or their employees, makes any warranty, express or implied, or assumes any legal liability or responsibility for the accuracy, completeness or usefulness of any information, apparatus, product or process disclosed, or represents that its use would not infringe privately owned rights.

TECHNICAL INFORMATION DIVISION
LAWRENCE BERKELEY LABORATORY
UNIVERSITY OF CALIFORNIA
BERKELEY, CALIFORNIA 94720